FINAL REPORT

ON

N.A.S.A. Contract NAS 9-13306

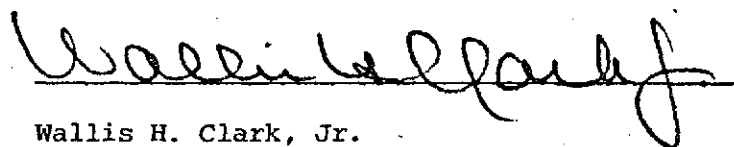March 15, 1973 to February 15, 1974

Wallis H. Clark, Jr.
Graduate Professor of Biology
Department of Biology
University of Houston
    and
Supervisory Research Biologist
National Oceanic and Atmospheric Administration
Gulf Coastal Fisheries Center
Galveston, Texas

I.

CONTRACT OBJECTIVES

A.   Fine structural examination of third stage <u>Nematospiroides</u> <u>dubius</u>
     larvae.

B.   Fine structural survey of the gametes, genital tracts, and the
     primordial cells of the gonads of mature <u>Nematospiroides</u> <u>dubius</u>.

II.

RESEARCH REPORT

A.   Third stage larvae of <u>Nematospiroides dubius</u>.

For this portion of the contract work the reader is referred to the
quarterly progress report on N.A.S.A. Contract NAS 9-13306, June 16
to September 15, 1973. Though further work was done on the larvae
no additional information was obtained that had not been previously
reported.

B.   Reproductive survey of <u>Nematospiroides</u> <u>dubius</u>.

1. Spermatogensis, the mature sperm, and sperm-egg association in
   <u>Nematospiroides</u> <u>dubius</u>.

INTRODUCTION

Sperm have customarily been grouped into two classes, the flagellated and nonflagellated. The nonflagellated sperm can be divided into three types: (1) vesiculiform (decapod crustacea and milmipedes), (2) tubuliform (ticks), and (3) amoeboid, found in nematodes (Nath, 1956). The latter can be round, conical, lobate, or elongate (Hyman, 1951), and all lack a flagellum and a distinct acrosome. While the nematode sperm differ markedly from the "typical flagellated" ones, many workers have attempted to homologize some of their cytoplasmic components with those of the flagellated sperm (Bowen, 1925; Stardivant, 1934; Collier, 1936; Nath and Singh, 1956; Hovasse, 1958; Foor, 1968 and 1970; Clark, 1972). For such homologies to be meaningful, thorough developmental studies are necessary. Unfortunately, such studies are sparse, and incomplete.

The only ultrastructural investigations concerned with nematode spermatogenesis are those of Favard (1961), Lee (1971), Pasternak and Samoiloff (1971), Beams and Sekhon (1972), and Neil and Wright (1973). Foor (1970) utilizing the electron microscopic studies available, divided the nematode sperm into four types: ascaroid, oxyuroid, dioctoptymoid, and stronglyloid. Since then, a new type, trichuroid, has been added (Neil and Wright, 1973).

Our knowledge of nematode sperm differentiation is fragmentary; because, of the 11 superfamilies of nematodes (Cheng, 1964), the information presently available covers only six. Most of the ultrastructural work done to date has been concerned with the ascaroid type (Favard, 1961; Clark et al, 1967, 1968, 1972; Foor, 1968, 1970, 1971, 1973, 1974; Lee, 1971).

Each of the other sperm types are represented by a single investigation: the oxyroid by Aspicularis tetraptera (Lee and Anya, 1967); the dioctophymoid by Dioctophymarenale (Foor, 1970); the trichuroid by Capillaria heptica (Neil and Wright, 1973); and the strongyloid by Nippostrogylus brasiliensis (Jamuar, 1966). Thus it is apparent that germ cell development has received little attention, and our major understanding of nematode spermatogenesis is based on a small number of investigations. Consequently, it is not feasible to describe a typical nematode sperm or give a generalized picture of sperm components and their role in reproduction.

For the above reasons, a thorough study of nematode spermatogenesis was initiated using the strongyloid Nematospiroides dubius as an experimental animal. This organism can be maintained in the intestine of the mouse, is easily handled, has a relatively short life cycle, and is often seen in copula.

MATERIALS AND METHODS

Nematosporoides dubius was maintained in the laboratory by cultivating the third larval stage from the fecal pellets of infected male mice (Cross, 1961). The larvae were inoculated periodically into C57B1-6 mice obtained from Texas Inbred Mice Company. Mature worms were isolated from the duodenum of infected mice and kept at 37°C in 0.85% NaCl (Sommerville and Weinstein, 1964). Male worms were distinguished under the dissecting microscope by their copulatory bursae. The reproductive tract was forcibly expelled from the body of the worm by making a cut about 3 mm anterior to the bursae.

Light Microscopy:

For vital staining, seminal vesicles were placed in 0.01% acridine orange in normal saline for 10 minutes. The tissues were then rinsed with normal saline, smeared on glass slides, and examined with a fluorescent dark field microscope (Clark et al, 1972).

Electron Microscopy:

Male and female reproductive tracts were placed in 3% glutaraldehyde buffered with eiterh 0.1 M phosphate at pH 7.3, or 0.1 M cacodylate at pH 7.3 with 6% sucrose added. After 1 hour in glutaraldehyde at room temperature, the tissues were washed with 0.1 M phosphate or 0.1 M cacodylate buffer, and postfixed with 1% osmium tetraxide in 0.1 M phosphate or 0.1 M cacodylate buffer at 4°C for 1 hour. The samples were then dehydrated in an acetone series, and embedded in a low-viscosity epoxy resin (Spurr, 1969). Ultrathin sections were obtained on a Porter-Blum MT2 ultramicrotome and mounted on 300 mesh uncoated grids. The sections were stained for 7 minutes with alcoholic uranyl acetate followed by lead citrate (Venable and Coggeshall, 1965). Sections were studied with an Hitachi H-S-8 or an AEI-EM 6B electron microscope. For light microscopy, sections were stained in 0.25% aqueous toluidine blue in 0.15% sodium borate.

OBSERVATIONS

Spermatogonia:

The spermatognoia, which are approximately 6 μ in diameter, are tightly packed within the testis. Like other cells undergoing

rapid protein synthesis and cytoplasmic growth, the spermatogonia contain numerous ribosomes. The cytoplasm contains rod-shaped mitochondria, a poorly developed endoplasmic reticular system, few Golgi bodies, lipid droplets, vacuoles which may contain fibrous material, and a few distinct microtubules (Figs. 1 and 1A). The nuclear volume is large relative to the volume of the cytoplasm. Within the nucleoplasm is a prominant nucleolus composed of a pronounced nucleonema. Chromatin, though found throughout the nucleoplasm, is often seen closely associated with the nucleoli (Fig. 1).

The surface of the spermatogonia adjacent to the testicular wall has finger-like projections which are about 200 A^o in diameter. Occasionally, these processes could be seen between adjacent spermatogonia (Fig. 1).

In more advanced spermatogonial stages, the rough endoplasmic reticulum becomes quite pronounced. The reticular cisternae appear scattered throughout the cytoplasm, and sometimes become engorged with electron dense material at one end while the other end becomes capsule-shaped (Fig. 2). This capsule encloses a mass of fibrillar material. Golgi bodies, each made of five to seven cisternae, and mitochondria, which look less elongated than those of early spermatogonia, appear to be in close contact with the encapsulated fibrillar material. At this stage, the chromatin material is quite dispersed, and the outer nuclear membrane shows continuity with the endoplasmic reticulum (Fig. 2).

Primary Spermatocytes:

Primary spermatocytes of N. dubius, in contrast to those of most nematodes studied to date are in cytoplasmic continuity with a

cytoplasmic, nucleated rachis which contains mitochondria, Golgi bodies, fibrous bodies and well developed endoplasmic reticulum. The plasma membranes of primary spermatocytes have numerous villus-like projections which are about 0.1 u in diamter. These processes may extend all the way between two neighboring spermatocytes (Figs. 3 and 4).

The primary spermatocytes are larger than the spermatogonia, and exhibit features of cells involved in active growth. They contain a large nucleus with dispersed chromatin and one or more nucleoli (Figs. 3 and 4).

Numerous mitochondria with large cristae, a highly branched endoplasmic reticular system distributed throughout the cytoplasm, and a large number of Golgi bodies per section are also typical features of this stage (Figs. 5 and 6). The fibrillar bodies have assumed a more distinct shape, though they have not completed their cytodifferentiation.

At this period of development the fibrillar bodies are composed of a bundle of fibrous strands closely associated with each other. Each fibrous element is about $50^{\circ}A$ in diameter and 0.3 u in length and is separated from its neighboring element by about $50^{\circ}A$. As mentioned earlier, each fibrous bundle is surrounded by a capsule-shaped extension of a hypertrophied segment of endoplasmic reticulum. The encapsulation of the fibrous bodies (Fig. 38) occurs during differentiation of these bodies when the free end of the capsule approaches the main body of the engorged reticular cisternae (Fig. 36) and apparently fuses with it (Fig. 37).

Concomitant with this stage of cytoplasmic differentiation are the meiotic divisions. The nuclear envelope is lost and chromosomes

become apparent. Microtubules are evident extending between the chromo-
somes and division centers (Figs. 5, 6, 7). The division centers are
electron dense regions containing conspicuous centriole pairs. These
centrioles are at 90° to each other and each consists of 10 triplet
sets of microtubules. The triplets are embedded in an electron dense
matrix and an electron opaque core (700°A in diameter) is present in
the middle of the centriolar cylinder. Each centriole is about 0.2 μ
in diameter and 0.4 μ long (Figs. 6, 8).

Cytokinesis does not take place until the meiotic divisions
are completed. As the divisions terminate, fibrous bodies, Golgi
bodies, mitochondria, and endoplasmic reticulum align along the planes
of the eventual cleavage furrows (Figs. 9, 10, 11, 12). As cyto-
kinesis ensues the leading edge of each furrow exhibits a thickening
or electron density (Fig. 10). At this stage the heterochromatin
is condensed and localized within the center of the future spermatids.
Microtubules radiate from these heterochromatic or nuclear regions
(Fig. 9). Incorporated with each nuclear region is a division center
(Figs. 9, 11). As cytokinesis is completed, each spermatid assumes
typical characteristics. At some point during meiosis, the rachis
terminates and the dividing cells become free of its confines.

Spermatids:

The spermatids are spherical-shaped cells characterized by
a centrally located condensed nucleus which lacks a nucleolus and a
nuclear enevelope. A pair of centrioles is present within a nuclear

fossa (Figs. 12, 13). Surrounding the nucleus is a cytoplasmic region void of organelles but containing numerous microtubules which appear to emanate from the nucleus (Figs. 12, 13). At the periphery of this void area are fibrous bodies, Golgi bodies and a few mitochondria. Between these organelles and the plamma membrane, dialated endoplasmic reticulum is very common. The fibrous bodies at this stage are very similar to those described in the spermatocytes (Figs. 12, 13).

Development of Spermatids:

One of the fundamental features of spermatid development is the invagination of one side of the nucleus. Early in this process the nucleus is round with a small fossa in which two centrioles are located (Fig. 13). With further invagination, the nucleus becomes "C" shaped (Fig. 13), then "U" shaped (Figs. 33, 34), and eventually it becomes "V" shaped (Figs. 15, 35). Concomitant with these changes in nuclear morphology, a change in the position of the nucleus takes place. In early stages of spermiogensis, the nucleus is centrally located, and as development proceeds it moves toward one pole of the cell where it remains during subsequent development (Figs. 14, 15, 16). In this position, the nucleus is very electron dense, filamentous, and is separated from the plasmalemma by a space of $600°A$ (Fig. 15). Throughout these changes in nuclear morphology, the centrioles remain associated with the nuclear fossa and usually occupy the area between the tips of the two nuclear arms (Figs. 16, 17).

Microtubules, approximately $240°A$ in diameter, which are randomly located in the cytoplasm of spermatids in earlier stages, assume a longitudinal orientation in the elongated spermatid (Figs. 14, 15, 17, 19). In addition, microtubules are seen in contact with the

outer membranes of the reticular elements which surround the fibrous bodies (Figs. 32, 33). During early spermiogenesis, the mitochondria and other cytoplasmic organelles remain static. However, as spermatid differentiation proceeds, concentration and migration of the endo-plasmic reticulum, ribosomes, and Golgi bodies to one side of the developing spermatid occurs. As these organelles condense at one pole, segments of endoplasmic reticulum separate them from the rest of the cell cytoplasm (Fig. 14). Once these components are isolated, the plasma membrane of the spermatid constricts around the nucleus (Figs. 15, 16). This constriction results in the loss of that portion of the cell containing the endoplasmic reticulum, ribosomes and Golgi bodies resulting in the formation of the cytophore (Figs. 15, 16, 20). During the above changes, the fibrous bodies retain their position around the peripheral cytoplasm, being separated from the plasma membrane by a space of 0.1 to 0.3 μ (Figs. 14, 15, 16, 17, 18, 19). The structure of these bodies in an elongated spermatid is similar to that in a younger spermatid, except for the appearance of membrane invaginations (Figs. 14, 15, 16, 17, 18, 19) which represent precursors of finger-like projections which appear in mature sperm. Some fibrous bodies have "umbrella" shaped blebs, about 0.3 μ in width, which are directed toward the plasma membrane of the developing spermatid (Figs. 15, 18, 19).

As described previously, microtubules run the length of the cell. These tubules are found in the central cytoplasm of the cell which is void of organelles. They extend from the base of the nucleus to the opposite pole or pseudopodial end of the elongated spermatid (Figs. 15, 17, 19, 21). This pseudopodial region contains small electron

dense granules, 0.1 μ in diameter, which appear to represent tubule termination points (Fig. 19). The pseudopodial cytoplasm contains no organelles and is limited externally by a convoluated region of plasma membrane (Figs. 19, 21).

Once the spermatids enter the seminal vesicle several noticeable changes take place. The fibrous bodies lose their fibrillar components and become distinct vesicles, 0.4 μ in diameter. The fate of the fibrillar material is in question. The limiting membranes of the vesicles form long finger-like invaginations which extend well into the vesicle's matrix (Figs. 23, 24, 25). These structures are similar to the proacrosomal vesicles described in the Ascarids (Favard, 1961; Clark et al, 1967, 1968, 1972). In some instances the vesicles have attached, via the blebs, to the plasmalemma and dehiscense has taken place (Fig. 24). Sperm released from the seminal vesicle and treated with acridine orange exhibit a bright green fluorescence in the nuclear region (Fig. 22). Also noted with this technique are small orange flouorescing bodies believed to be the vesicles (Fig. 22).

Other distinct features of sperm from the seminal vesicle are the presence of electron dense cytoplasmic inclusions and a bulbous pseudopodium at one pole of the cell (Figs. 22, 23, 25). The pseudopodial cytoplasm contains microfilaments, 60°A in diameter and microtubules (Fig. 25).

Sperm From the Female Tract:

Upon entering the female genital tract sperm become extremely polymorphic. Their cellular morphology ranges from elongated (Fig. 29),

as described for sperm from the male, to oval-shaped (Fig. 26). A
very interesting feature is the presence of a cytoplasmic collar which
extends around the nucleus (Figs. 27, 28). Other distinct cytoplasmic
features include large amorphous bodies found in the cytoplasm, which
in many instances are closely associated with the nuclear region (Fig.
26), and elongated mitochondria which often "wrap" around the vesicles
(Figs. 26, 27, 29).

In many instances dehisced vesicles exhibit collar-like
thickenings at their junction with the sperm plasmalemma (Figs. 26,
29, 40). Microtubules are still present in the elongated sperm and
extend from the nuclear fossa into the pseudopodial cytoplasm (Fig. 31).
Occasionally some sperm exhibit more than one fibrous pseudopodial
process (Figs. 30, 39A).

Often cross sections through the seminal receptical region
of the female genital tract reveal sperm in close association with
eggs. These spermatozoa exhibit distinct structural changes. Their
nuclei appear to be decondensing and becoming fibrillar in nature
(Fig. 42). Also their vesicular bodies become crescent or "donut"
shaped and contain an electron dense material (Figs. 41, 42).

DISCUSSION

Although the scheme of sperm differentiation in N. dubius is, in many respects, in accord with the picture of spermatogenesis in other nematodes, this organism has unique spermatogenic features. For example, spermatogonia and primary spermatocytes, unlike those of other nematodes investigated (Neil and Wright, 1973), do not appear to be attached by cytoplasmic bridges, but instead are attached to a cytoplasmic, nucleate rachis, a feature reported in only one other nematode (Lee, 1971). Secondary spermtaocytes are connected by cytoplasmic bridges, a trait suggested to play a role in synchronization of the spermatogenic cycle (Fawcett, 1961; Dym and Fawcett, 1971).

A typical feature of nematodes having the ascaroid type sperm is the presence of refringent bodies or cones. These were first described by Van-Beneden and Julin (1884). Recent investigators have suggested the presence of RNA in these inclusions (Nath et al, 1961). However, Clark et al (1972) agree with Panijel (1950) that the refringent bodies are made of "an acid protein of high nitrogen content, rich in aspartic acid, and linked to a purine ring". Although in N. dubius neither germ cells nor sperm from seminal vesicles possess refringent bodies or cones, sperm taken from the female genital tract have clumps of amorphous, particulate material in the vicinity of the nucleus.

Organelles typical of nematode germ cells undergoing spermatogenesis and a subject of controversy among investigators are the vesicular bodies, or proacrosomal vesicles (Favard, 1961; Clark et al, 1967, 1968, 1972). These organelles are present in the peripheral cytoplasm

of most nematode sperm thus far studied. They were first described by
Favard (1961), who reported that they were of Golgi origin and called
them "Golgi hats" or proacrosomal vesicles, but did not ascribe any
function to them. Januar (1966) reported mitochondria-like inclusions
in N. brasiliensis sperm which he described as superficially resembling
mitochondria and staining with Janus green. However, he did not deter-
mine the origin of these inclusions. In a fine structural study, Clark
et al (1967) described membrane-bound vesicles having whorls of fibrillar
material and finger-like projections in their matrices. Later in 1972,
the same authors cytochemically demonstrated that these vesicles are
positive for the periodic-acid·schiff and acid phosphatase reactions
and dehisce before fertilization. It is worth mentioning that these
authors reported that the vesicles dehisce only in sperm recovered from
the female genital tract. Foor (1968, 1970) described similar vesicles
in A. lumbricoides which he called "membrane specializations", assuming
them to be of mitochondrial origin. According to Foor (1968, 1970)
some of these vesicles break open (dehisce) in sperm from the seminal
vesicle. For the above reasons he did not believe the vesicles were pro-
acrosomal in nature. Beams and Sekhon (1972) presented ultrastructural
evidence that these vesicles are of Glogi origin. This opinion is
shared by Pasternak and Samioloff (1971), who called the vesicles
c-bodies and v-bodies.

The present work provides evidence that the vesicles in
question are of endoplasmic reticular origin. Primoridia of these
vesicles become apparent in late spermatogonia as masses of fibrous
elements surrounded by endoplasmic reticular cisternae. The cisternae,
in primary and secondary spermatocytes, encircle the fibrillar elements
and hypertrophy at one side. The closeness of Golgi-bodies to the sites

of formation of the fibrous elements suggest that the Golgi complexes
are associated with the production of these structures. At the
spermatic stage, precursors of finger-like projections appear in the
engorged cisternal elements (vesicle); in sperm taken from the
seminal vesicle the fibrous elements are missing, and the interior of
the vesicular bodies is occupied by microvillus-like projections.
Some of these vesicles are shown dehiscing. The vesicles appear
attached to the sperm plasma membrane by necks or membrane thickenings.
Vesicular bodies of sperm recovered from the female genital tract show
the same features just described. The dehiscence of vesicles as
described in N. dubius sperm has been noted in other nematode sperm by
several authors (Favard, 1961; Jamuar, 1966; Clark et al, 1967, 1968,
1972; Foor, 1968, 1970, 1974; Beams and Sekhon, 1970, 1972; Lee, 1971;
Pasternak and Samioloff, 1971; Wright et al, 1973).

Clark et al (1972), believing the vesicles to be of Golgi
origin, exhibiting histochemical characteristics common of acrosomes
and dehiscing in the female genital tract, suggested that the vesicles'
secretory product might be essential in providing an environment neces-
sary for fertilization. Segments of the present investigation support
this hypothesis while other portions detract from it. The present
investigation has implicated the endoplasmic reticulum in vesicle
formation. This is interesting since several recent investigations
have demonstrated a distinct role of the endoplasmic reticulum in
acrosome morphogenesis (Franklin, 1971). The present study has also
shown an unquestionable change in vesicular structure in sperm closely
apposed to an egg surface. On the other hand, this work has also
demonstrated dehisced vesicles in sperm from males. Unfortunately,
vas sperm are very difficult to fix, leaving questions in the author's
mind concerning the validity of this dehiscence. Before the true signi-
ficance of these vesicles can be determined their isolation and bio-
chemical characterization must be completed.

The nucleus of N. dubius sperm undergoes a dramatic change
in shape and structure in the course of spermiogenesis. Early in this
process, the nucleus is composed of diffuse chromatin. It becomes
dense and fibrous in late spermatids, and very compact and electron
dense in mature sperm. Initially, a fossa is formed in one side of
the spermatid nucleus. Later in spermiogenesis the invagination becomes
more pronounced so that the centrally located "C"-shaped nucleus be-
comes "U"-shaped in late spermatids, and eventually polar and "V"-
shaped in mature sperm. Of the nematode species thus far studied, only
N. brasiliensis (Jamuar, 1966) exhibits similar nuclear changes. As
reported in other nematodes (Jamuar, 1966; Clark et al, 1967, 1972),
the N. dubius sperm nuclei lack a nuclear envelope.

A unique feature of the sperm of this parasite is the pres-
ence of centrioles composed of 10 triplets. In N. brasiliensis
(Jamuar, 1966) the centrioles are made of a core surrounded by a circle
of 18 "rods", and in C. hepatica (Neil and Wright, 1973) and A. caninum
(Foor, 1970) the centrioles have been reported to consist of 9 single
tubules only. Centrioles have not been reported in sperm of A.
lumbricoides (Foor, 1970), D. californicum (Wright et al, 1973), and
Diocytophyma sp. (Foor, 1970).

The microtubules in most nematode spermatocytes (except in
Aspicularis) are progressively lost during the final stages of matura-
tion (Foor, 1970). Only a few scattered microtubules are observed
during early spermatogenesis in N. dubius. However, during spermio-
genesis these tubules increase in number and radiate around the spermatid
nucleus. The microtubules extend from the nuclear region and assume
a parallel arrangement along the longitudinal axis of the maturing sperm
just prior to cytophore shedding. During this period of cyto-
differentiation the nucleus assumes its final shape. These microtubules

now appear restricted to the fossa region of the nucleus. Jamuar (1966) reported similar orientations of microtubules during spermiogenesis in N. brasiliensis, and Lee Anya (1967) described longitudinal bundles of microtubules in Aspicularis sperm. The fact that the microtubules become aligned around the inner margin of the nuclear fossa and retain this alignment throughout spermiogenesis, tends to suggest that the microtubules are associated with initiating and further accentuating the nuclear concavity. In addition the longitudinal orientation of microtubules in differentiating sperm strongly suggest that these tubules are important not only as elements needed for the morphogenesis of developing gametes, but also as significant factors in maintaining the final shape of N. dubius sperm. In the next chapter, the role of microtubules in development and maintenance of sperm shape will be further explored by using the drug cochicine.

The shedding of cytoplasmic remnants from maturing nematode sperm has been reported by several investigators (Van Beneden, 1884; Sturdivant, 1934; Miller, 1966; Nath et al, 1956; Foor, 1970; Kanwat, 1971; Neil and Wright, 1973). However, the only fine structural study showing cytophores and shedding of cytophore remnants is that of Favard (1961). The present work provides further information on this aspect of nematode sperm differentiation. In N. dubius the first step in the formation of the cytophore is the migration of endoplasmic reticulum cisternae, Golgi bodies and ribosomes from a mid-cytoplasmic position in spermatocytes to a peripheral one in spermatids. Later in spermiogenesis, these structures move in the direction of nuclear migration, and eventually are separated from the nucleus by endoplasmic reticulum. This phenomenon by which the nematode sperm rid themselves of excessive material is similar to that of the mammalian sperm (Bishop and Walton, 1960).

After copulation sperm undergo marked structural changes in the female genital tract. In elongated sperm the cap-shaped pseudopodial pole is lost and this pole of the sperm becomes actively amoeboid. This change in the pseudopodial area has been described in other nematodes (Foor, 1970, 1971, 1974) and is believed to help sperm travel down the female genital tract. In other instances globular sperm which lack microtubules have been observed. These findings are in agreement with the light microscopic study of Sommerville and Weinstein (1964) in N. dubius as well as other studies by Foor (1968, 1970, 1973, 1974) in other nematodes. Unfortunately the significance of these morphological changes are not fully understood. Whether the globular cells are mature sperm or activated cells no longer capable of fertilization is in question.

Fig. 1   An electron micrograph of a spermatogonium. Endoplasmic
          reticulum (ER), mitochondria (M), nucleus (N), nucleolus (nu),
          microtubules (arrows in insert), and lipid droplets (L) are
          shown. Arrow points to spermatogonial processes.

                                                              X 10,000

Fig. 1A. An electron micrograph illustrating microtubules in a
          spermatogonium (arrowhead).

                                                              X 40,000

Fig. 2.   An electron micrograph of an advanced spermatogonium.
          Continuity of endoplasmic reticulum (ER) with outer nuclear
          membrane (NM), fibrillar material (FM), Golgi bodies (G),
          and mitochondria (M) are demonstreated. Small arrowhead
          points to the capsular end of the endoplasmic cisternae and
          large arrowhead shows the engorged portion.

                                                              X 24,000
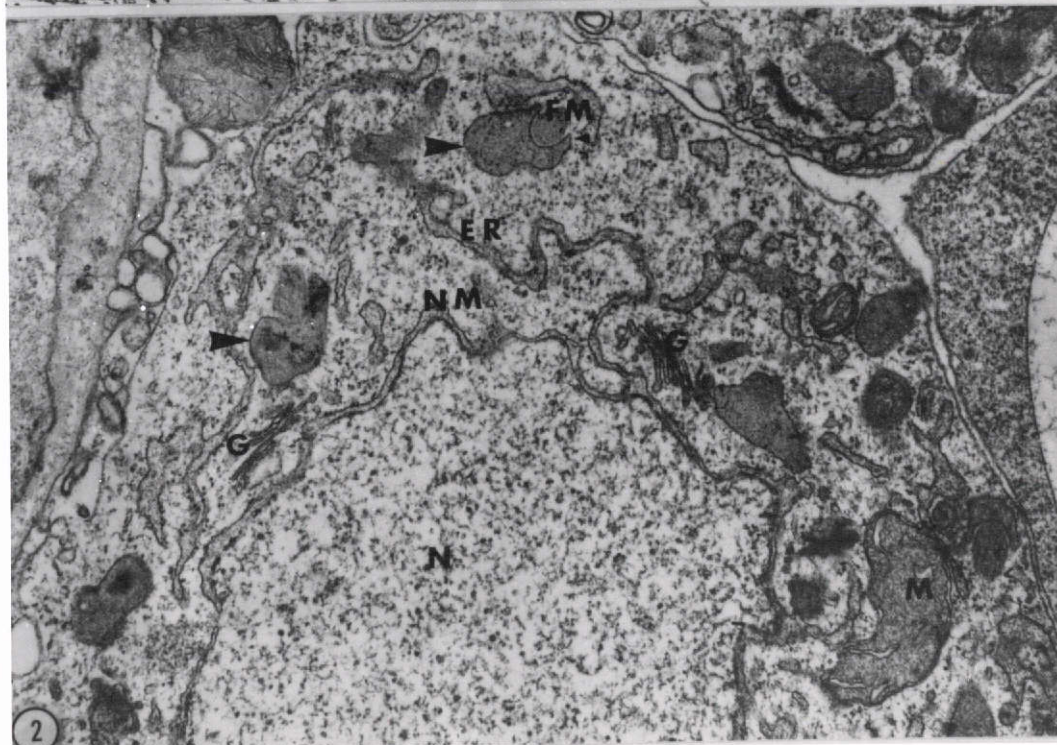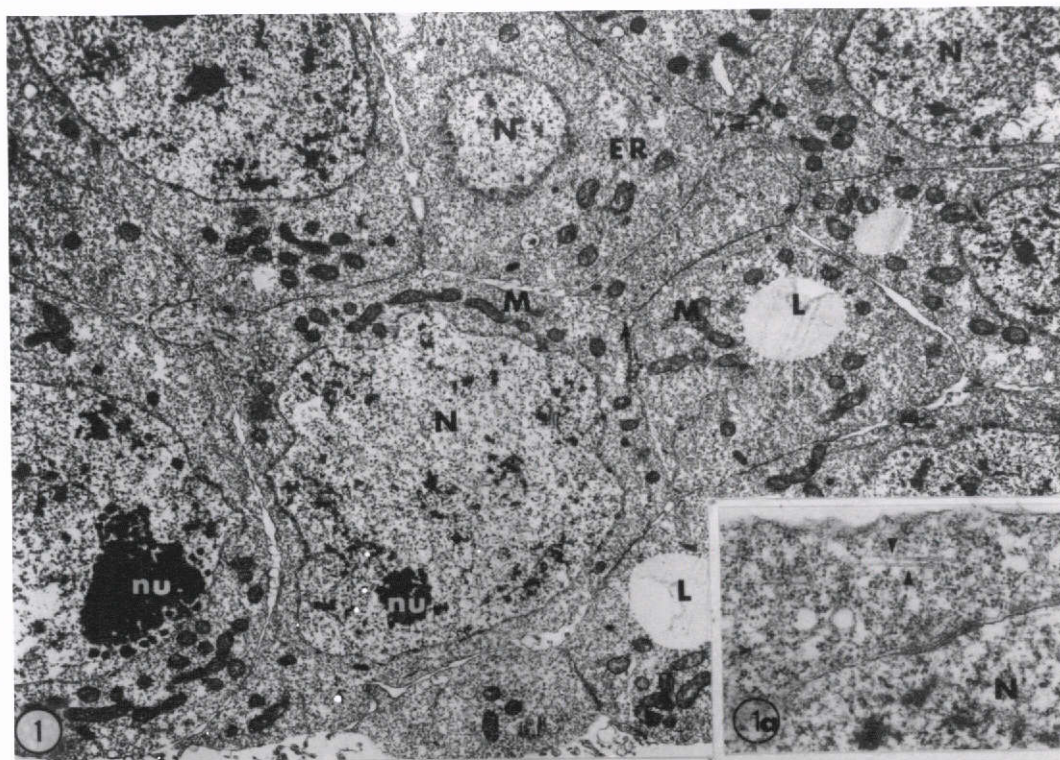
Fig. 3.   An electron micrograph showing a longitudinal section of
          a rachis (R) and primary spermatocytes (ps). Fibrous
          bodies (FB), Golgi bodies (G), endoplasmic reticulum (ER),
          mitochondria (M), a nucleus (N), and spermatocyte processes
          (P) are shown.

                                                          X 10,000

Fig. 4   An electron micrograph of a primary spermatocyte showing a
          nucleus (N), a nucleolus (Nu), fibrous bodies (B),
          mitochondria (M), and endoplasmic reticulum (ER). Arrow-
          head points to processes between primary spermatocytes.

                                                          X 10,000
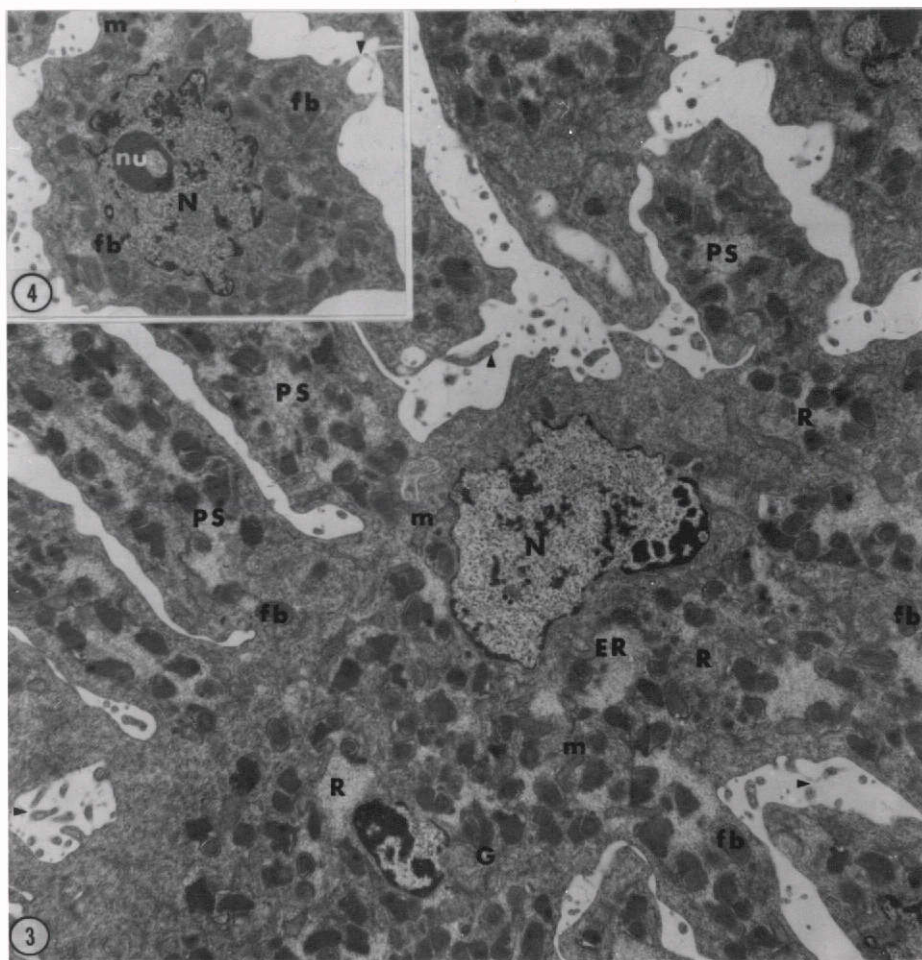
Fig. 5.   An electron micrograph of a primary spermatocyte. Fibrous

bodies (FB) with hypertrophied portion (large arrowhead).

Golgi bodies (G), endoplasmic reticulum (ER), mitochondria

(M), chromosome (CM), microtubules (small arrowhead), and

division center (DC) are shown.

X 16,800
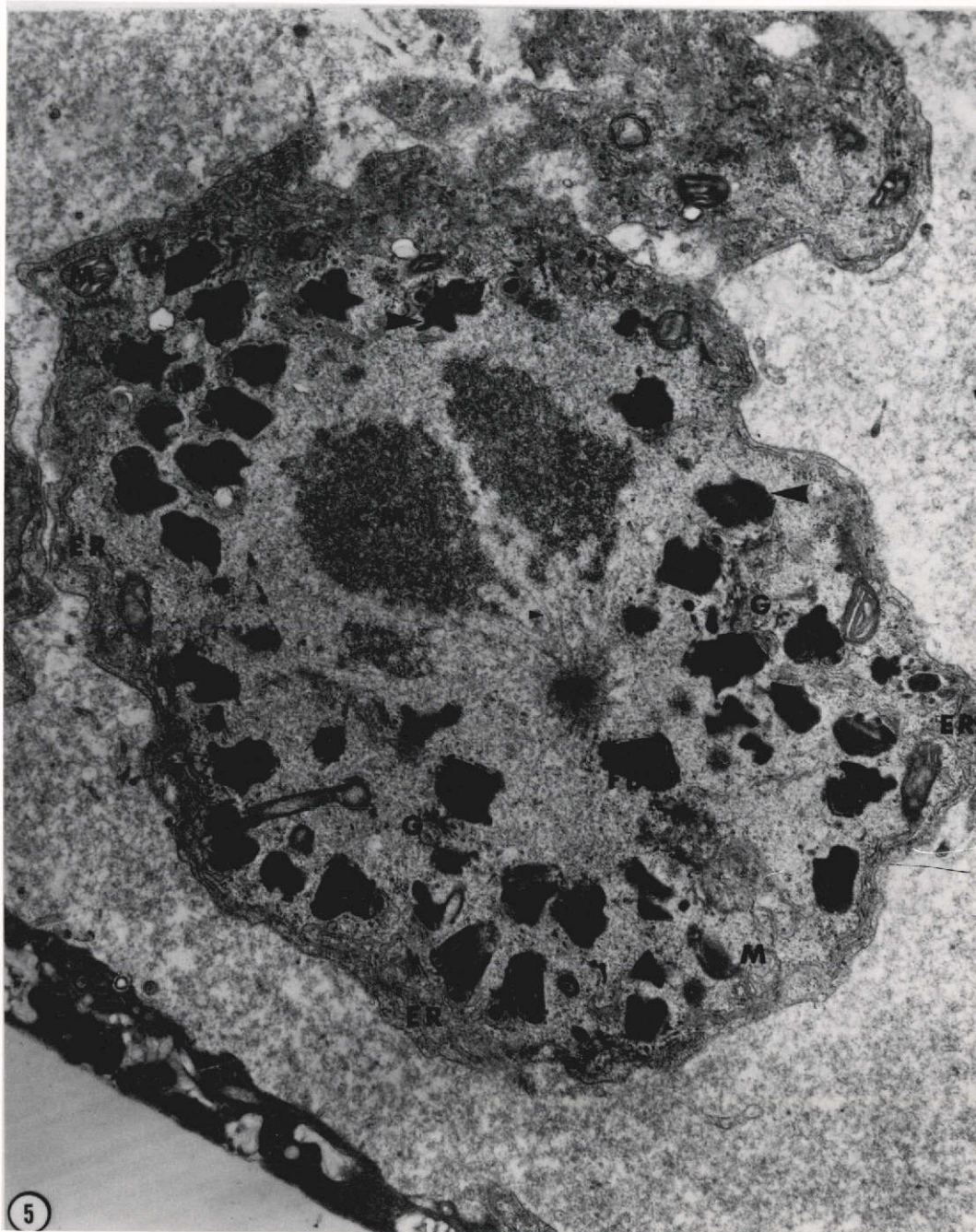
Fig. 6. An electron micrograph of a primary spermatocyte showing
Golgi bodies (G), fibrous bodies (FB), endoplasmic reticulum
(ER), mitochondria (M), centriole (C), a chromosome (CM),
and microtubules (arrowhead).

X 26,000

Fig. 7. An electron micrograph of a division center (DC), microtubule
(arrowhead), and chromosomes (CM).

X 30,000

Fig. 8. An electron micrograph showing two centrioles (C). The
lower centriole illustrates 10 triplets.

X 60,000

Fig. 9.   An electron micrograph showing two secondary spermatocytes.
Notice alignment of endoplasmic reticulum (ER), fibrous
bodies (FB), and Golgi bodies (G) along plane of cleavage
furrow. Microtubules (MY) and a nucleus (N) are also shown.

X 18,000

Fig. 10.   An electron micrograph showing thickenings (arrow) at the
leading edge of each furrow between two secondary spermato-
cytes.

X 12,000

Fig. 11.   An electron micrograph illustrating four secondary spermato-
cytes. Heterochromatin material (HC), a division center (DC),
fibrous bodies (FB), mitochondria (M), and endoplasmic reticulum
(ER) are shown.

X 8,600
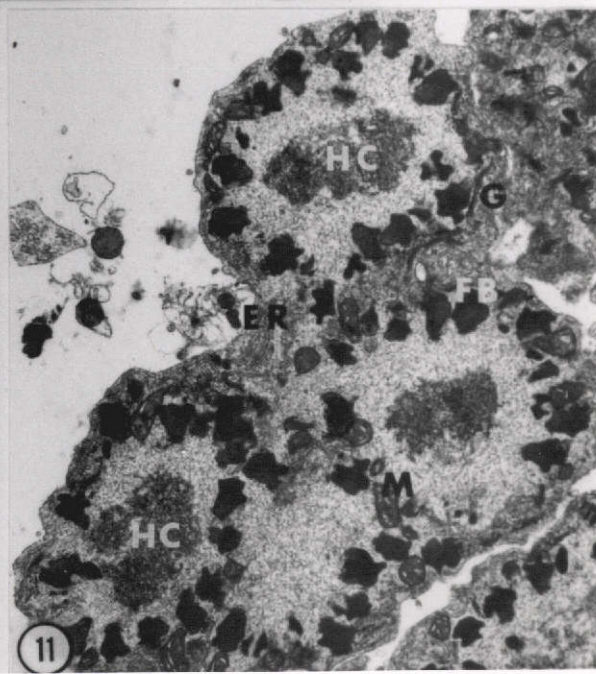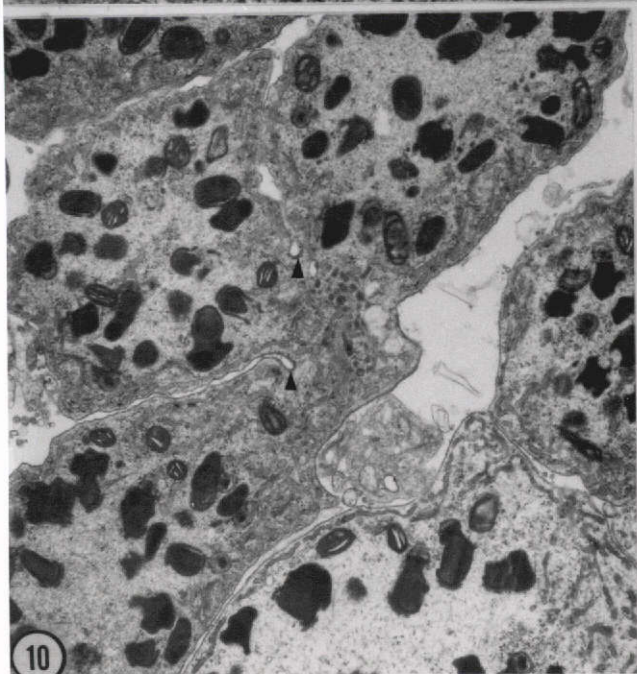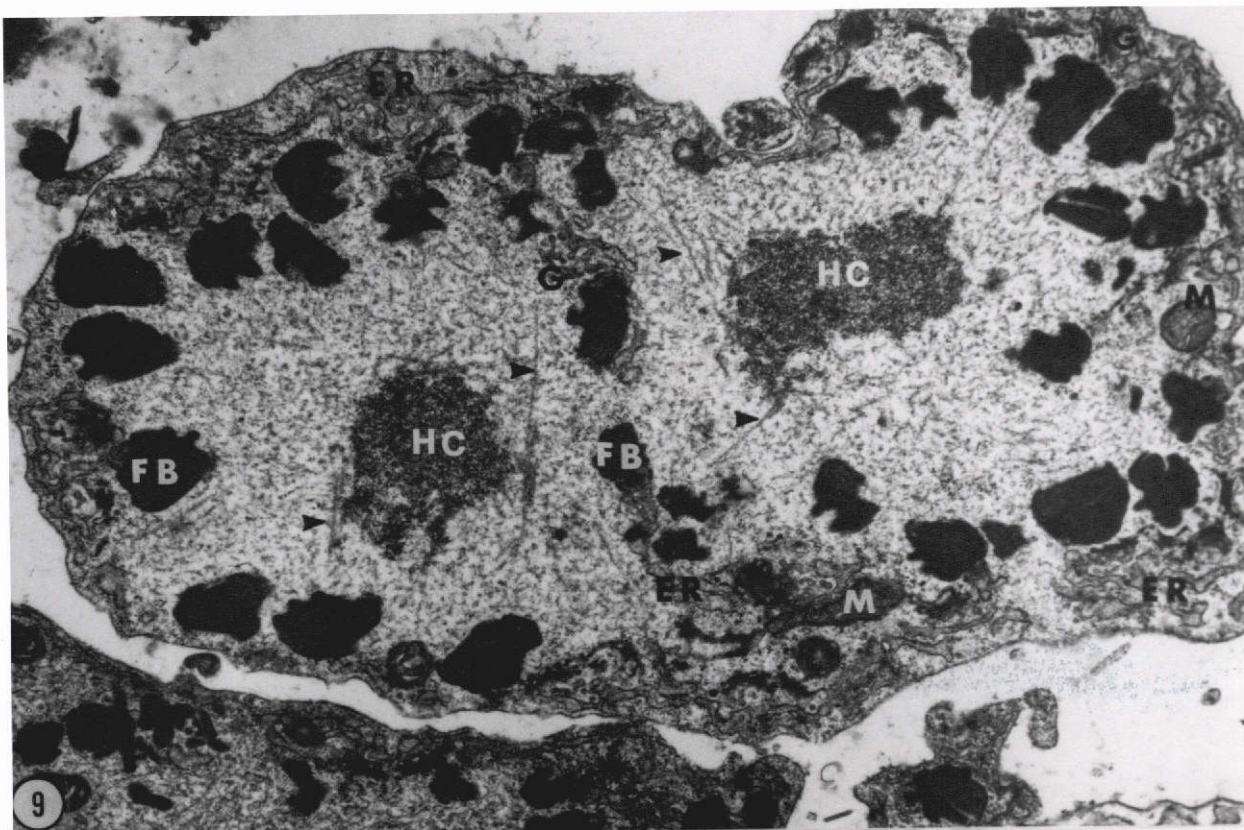
Fig. 12. An electron micrograph showing a spermatid. A centriole (C),
microtubules (MY), fibrous bodies (FB), Golgi bodies (G),
mitochondria (M), a nucleus (N), and endoplasmic reticulum
(ER) are illustrated.

X 21,000

Fig. 13. An electron micrograph showing a spermatid nucleus (N).
Embedded in the nuclear fossa are two centrioles (C), and
microtubules (MT), which radiate between the nucleus and
peripheral cytoplasmic organelles.

X 45,000
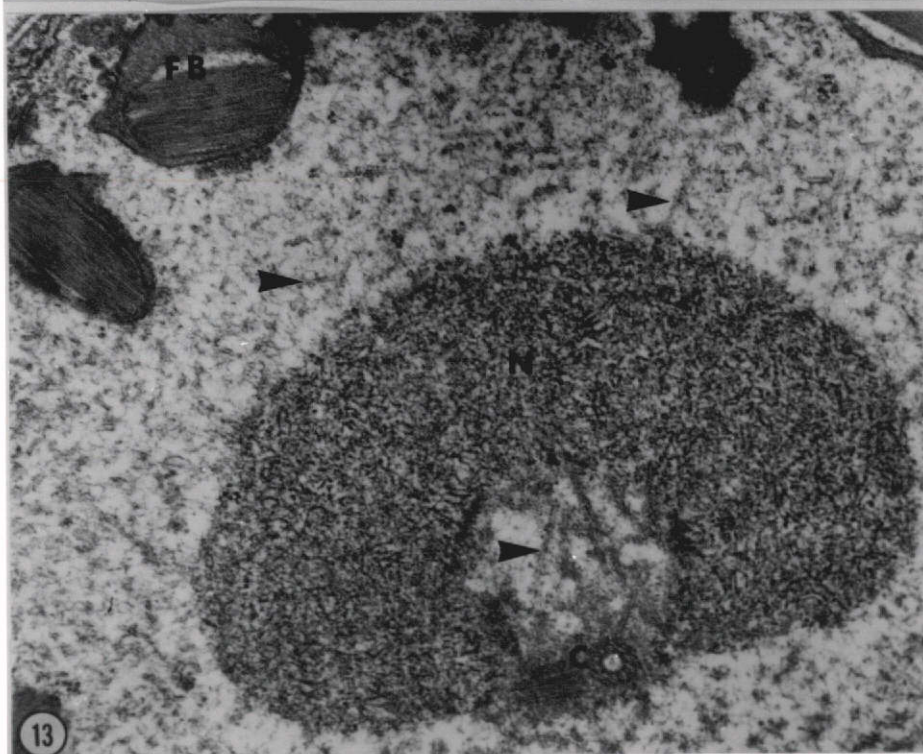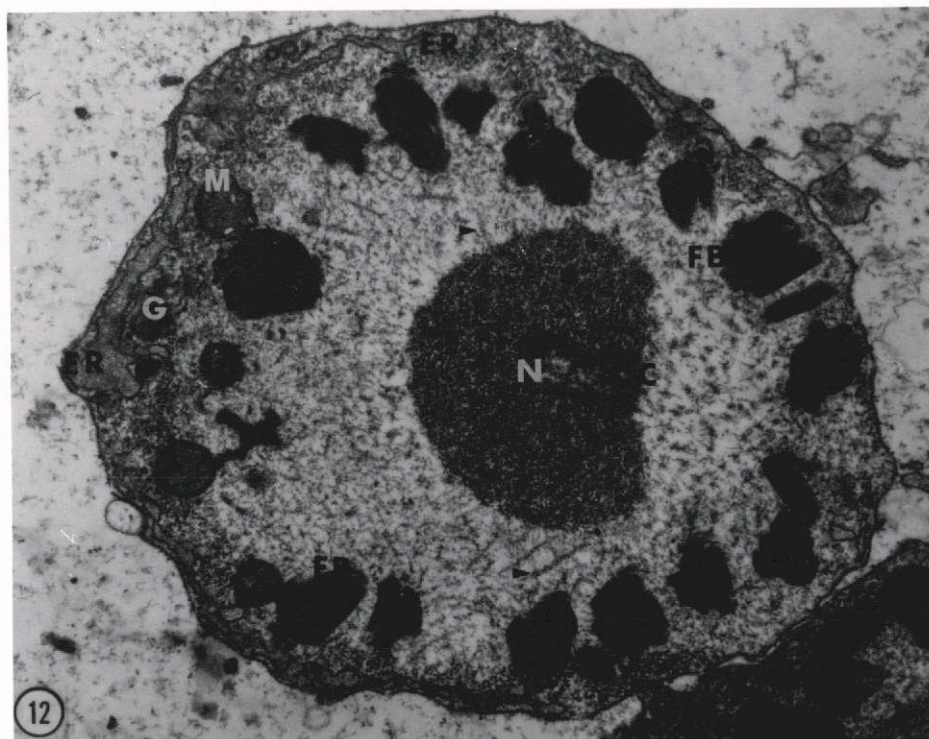
Fig. 14.   An electron micrograph demonstrating an elongated spermatid
with a cytophore (CP) containing Golgi bodies (G), endoplasmic
reticulum cisternae (ER), and ribosomes (r). Also shown are
the nucleus (N), microtubules (MY), mitochondria (M), and
fibrous bodies (FB). Arrows show membrane invaginations
of the hypertrophied portions of the fibrous bodies.

X 30,000

Fig. 15.   An electron micrograph showing an elongated spermatid about
to slough its cytophore (CP). An electron dense nucleus (N),
microtubules (MY), and fibrous bodies (FB) are demonstrated.
Small white arrows point to membrane invaginations in engorged
portion of fibrous bodies; large arrow points to blebs of
engorged parts of fibrous bodies.

X 15,000

Fig. 16.   An electron micrograph showing a nucleus (N), a cytophore (C),
and two centrioles (C) of an elongated spermatid.

X 10,000

14

15

Fig. 17. An electron micrograph demonstrating an elongated spermatid
which has sloughed its cytophore. Structures shown include
a nucleus (N), a centriole (C), microtubules (small black
arrowhead), vesicular bodies (VB) with inner membrane in-
vaginations (small white arrowhead), extruded fibrillar
elements (fe), mitochondria (M), and blebs (large arrows).

X 15,000

Fig. 18. An electron micrograph showing a vesicular body with finger-
like projections (arrows) and a bleb (b) in close junction
with plasmalemma (PL).

X 50,000

Fig. 19. An electron micrograph showing a portion of an elongating
spermatid with a nucleus (N), vesicular bodies (VB) which
contain inner membrane invaginations (small arrows) and
blebs (large arrows). Also shown are microtubules (small
black arrowhead) with their possible termination sites (large
black arrowhead) and convoluted boundary of pseudopodial
pole.

X 32,000
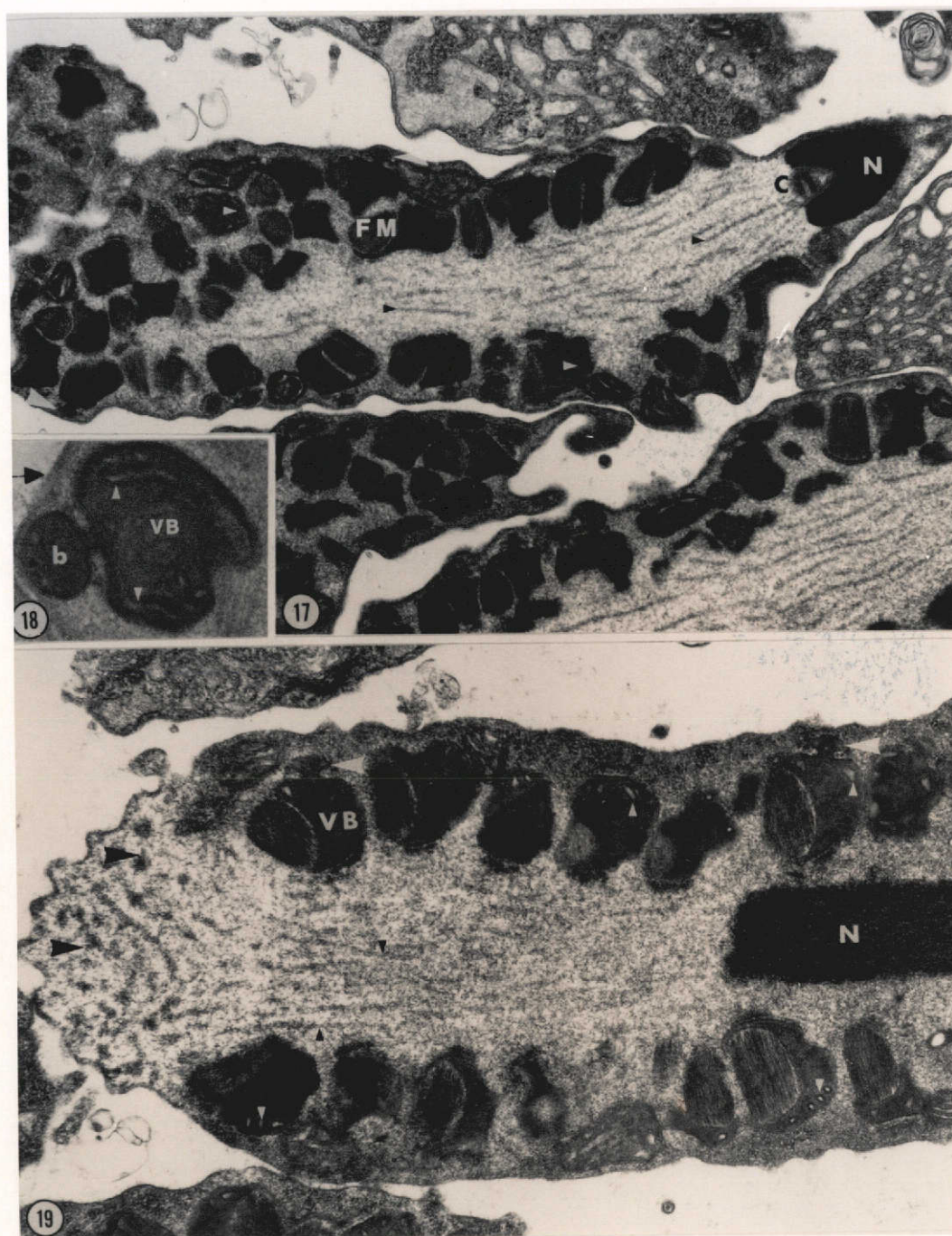
Fig. 20. An electron micrograph through a cytophore. Dilated endo-
plasmic reticulum (ER), Golgi bodies (G), and ribosomes (r)
are shown.

X 40,000

Fig. 21. An electron micrograph demonstrating the convoluted
boundary (large arrows) of the pseudopodial end of an
elongated sperm. In the vicinity of this pseudopodial area
are microtubules (small black arrowheads), and fibrous
elements (f). Vesicular bodies (VB) with inner finger-
like processes (small white arrowheads) and mitochondria
(M) are shown.

X 40,000
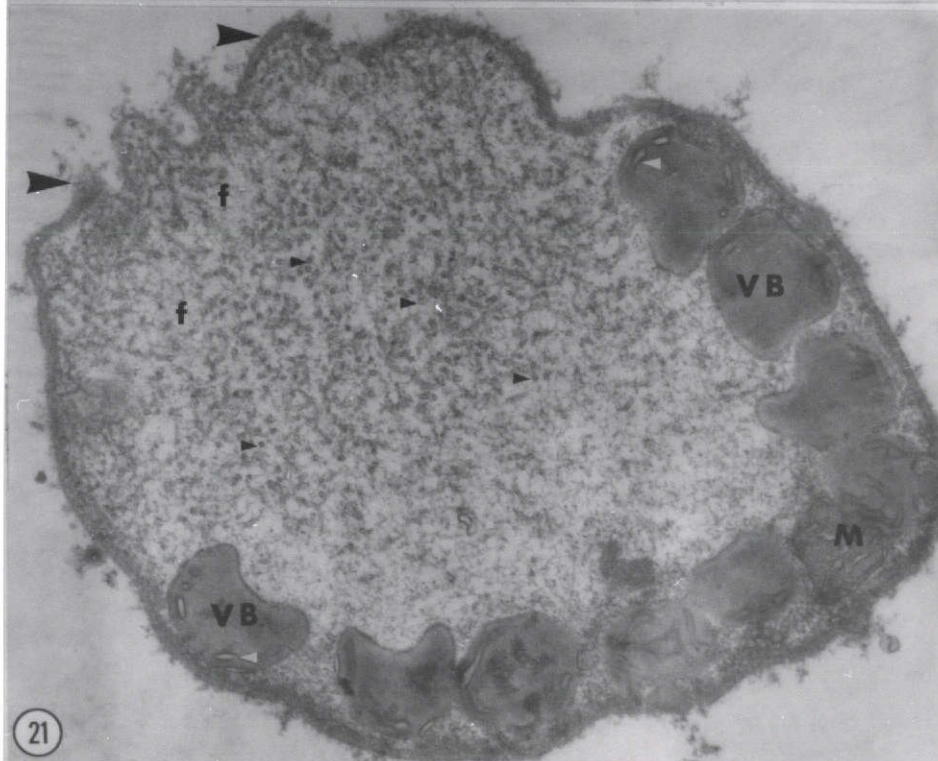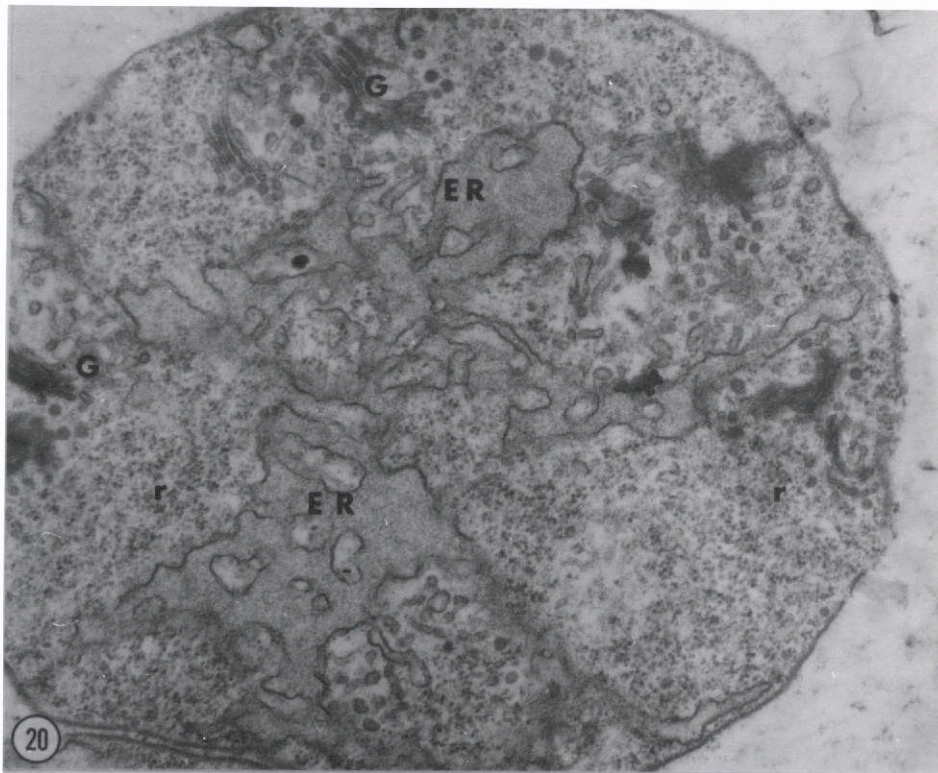
Fig. 22. A light micrograph (phase contrast) showing a sperm taken
from the seminal vesicle. The pointed, "V" shaped structure
is the nucleus (N); the cap-like part is the pseudopodial pole
(PP). The dark, bead-like structures (white arrowheads)
are presumably the vesicular bodies.

X 2,800

Fig. 23. An electron micrograph demonstrating a sperm in the seminal
vesicle. A portion of the nucleus (N), vesicular bodies (VB),
lipid-like droplets (L), and pseudopodial pole (PP) are seen.
Arrow points to a dehiscing vesicular body.

X 13,000

Fig. 24. An electron micrograph showing a section through the body of
a sperm taken from seminal vesicle. Notice finger-like pro-
jections in the vesicular bodies (VB); also junction of
dehiscing vesicular bodies with plasmalemma (small arrows).

X 42,000

Fig. 25. An electron micrograph through the pseudopodial portion (PP)
of a sperm in the seminal vesicle. Microtubules in cross
section (small arrows), and vesicular bodies (VB) are evident.

X 33,000

Figure 22: n, PP

Figure 23: N, L, VB, VB, PP

Figure 24: VB, VB, VB

Figure 25: VB, PP
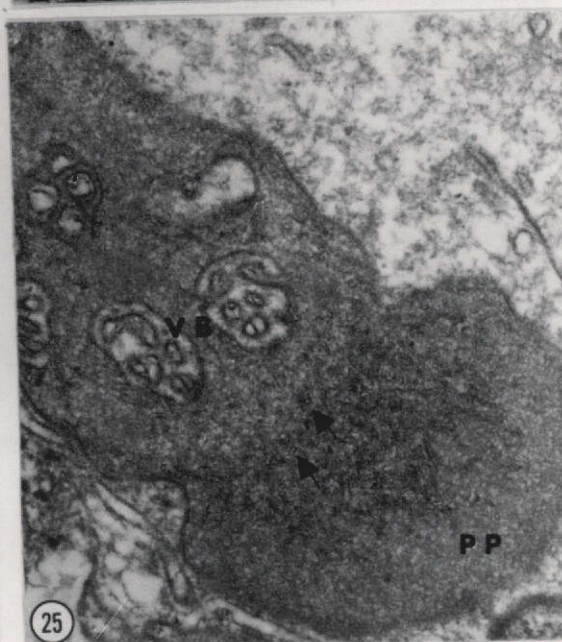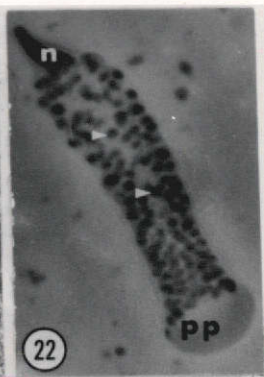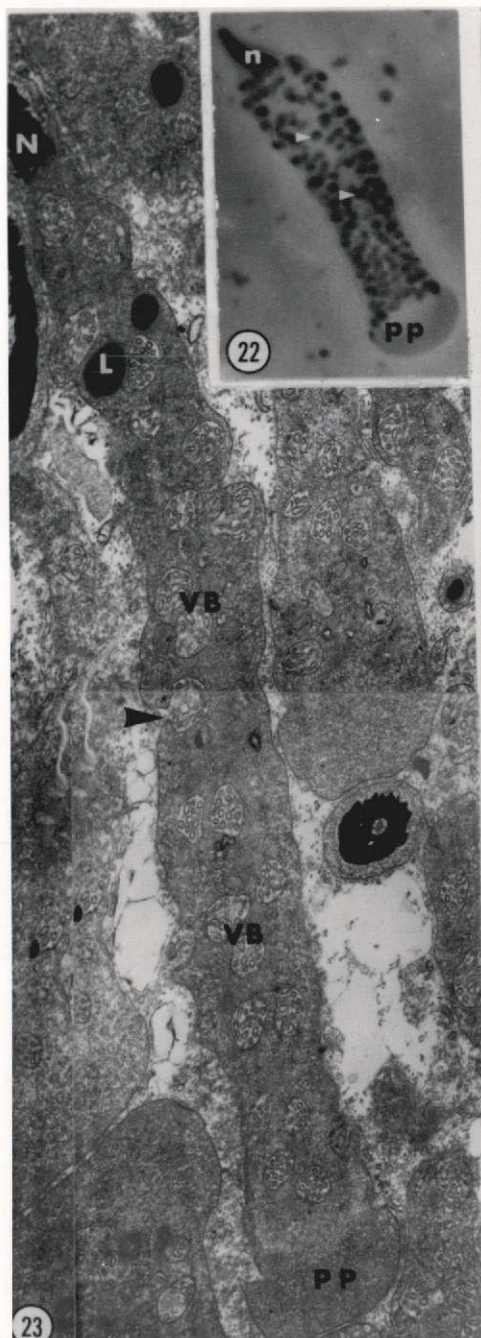
Fig. 26.   An electron micrograph demonstrating an oval-shaped sperm in
the female genital tract.   Notice the nucleus (N), amorphous
bodies (AB), vesicular bodies (VB) with inner finger-like
projections, collar-like thickenings (small arrows) at
junctions of vesicular bodies with plasmalemma, mitochondria
(M), and pseudopodial end (PP).

X 40,000

Fig. 27.   An electron micrograph showing a cytoplasmic collar (C)
around the nucleus (N) of a sperm in the female genital tract.

X 14,000

Fig. 28.   An electron micrograph through the nuclear pole of a sperm
in the female reproductive tract.   A nucleus (N), a centriole
(C), vesicular bodies (VB) and a cytoplasmic process (CP)
around the nucleus are shown.

X 28,000

Fig. 29.   An electron micrograph of an elongated sperm seen in the
female genital tract.   A pointed nucleus (N), amorphous body
(AB), vesicular bodies (VB), with collar-like thickenings
(arrowhead) at their fusion points with the plasmalemma, and
a fibrous pseudopodial area (PP) are demonstrated.   The
sperm is shown lying adjacent to a uterine wall (UW).

X 2,400
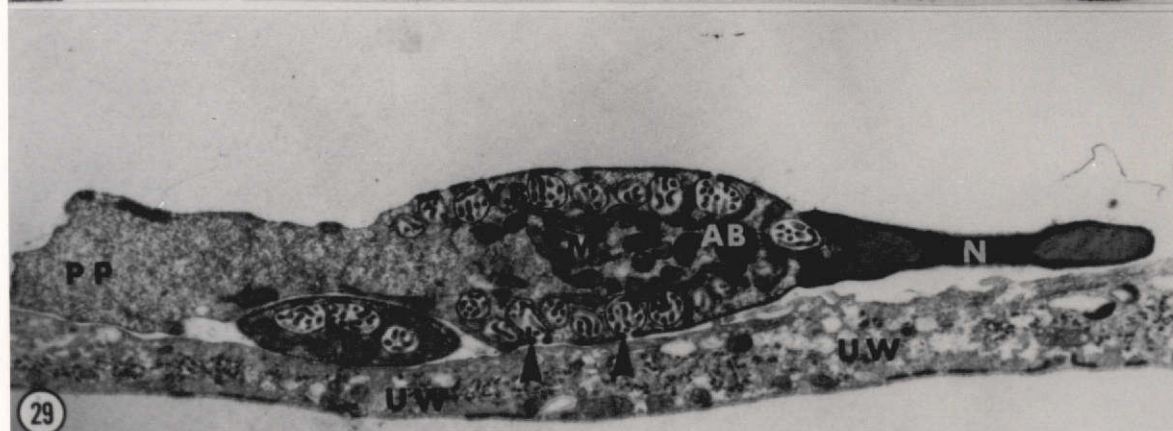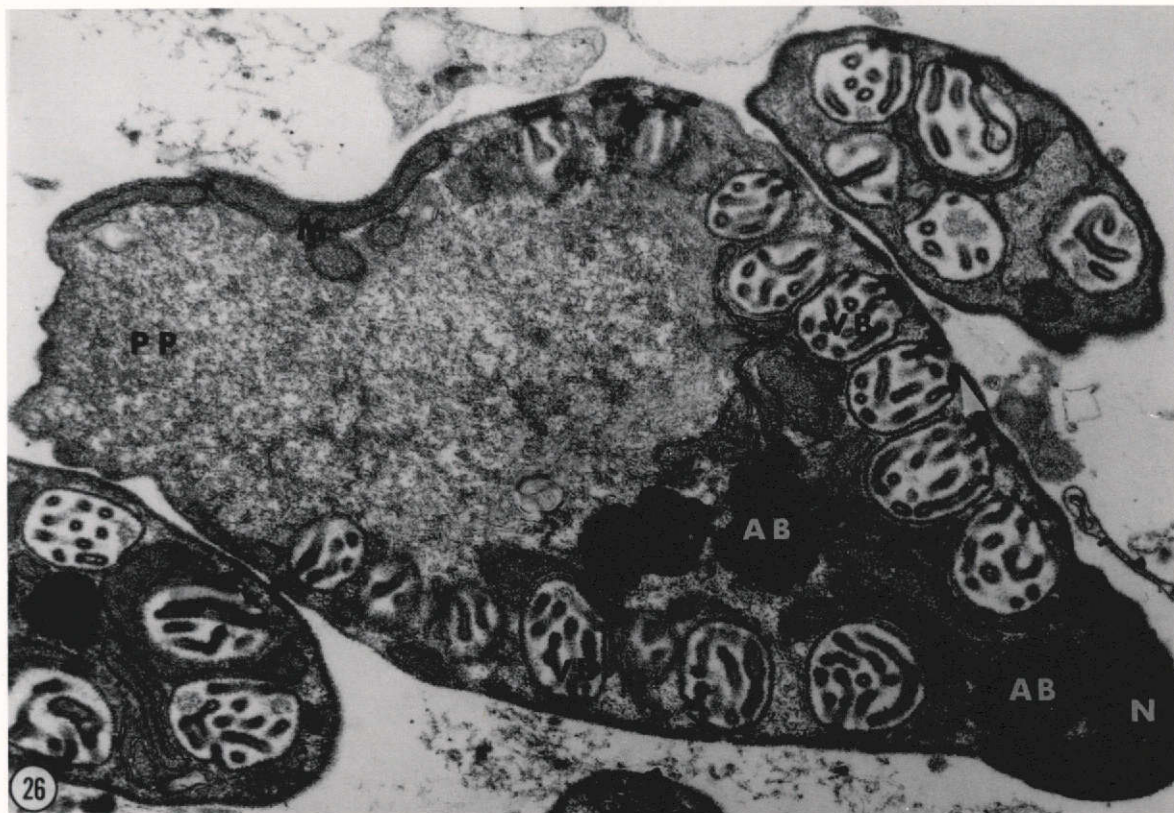
Fig. 30.   An electron micrograph of two pseudopodial processes (PP)
           of a sperm from the female reproductive tract.   Vesicular
           bodies (VB) which may be dehiscing in some cases (arrow-
           heads), and mitochondria (M) are shown.

                                                          X 18,000
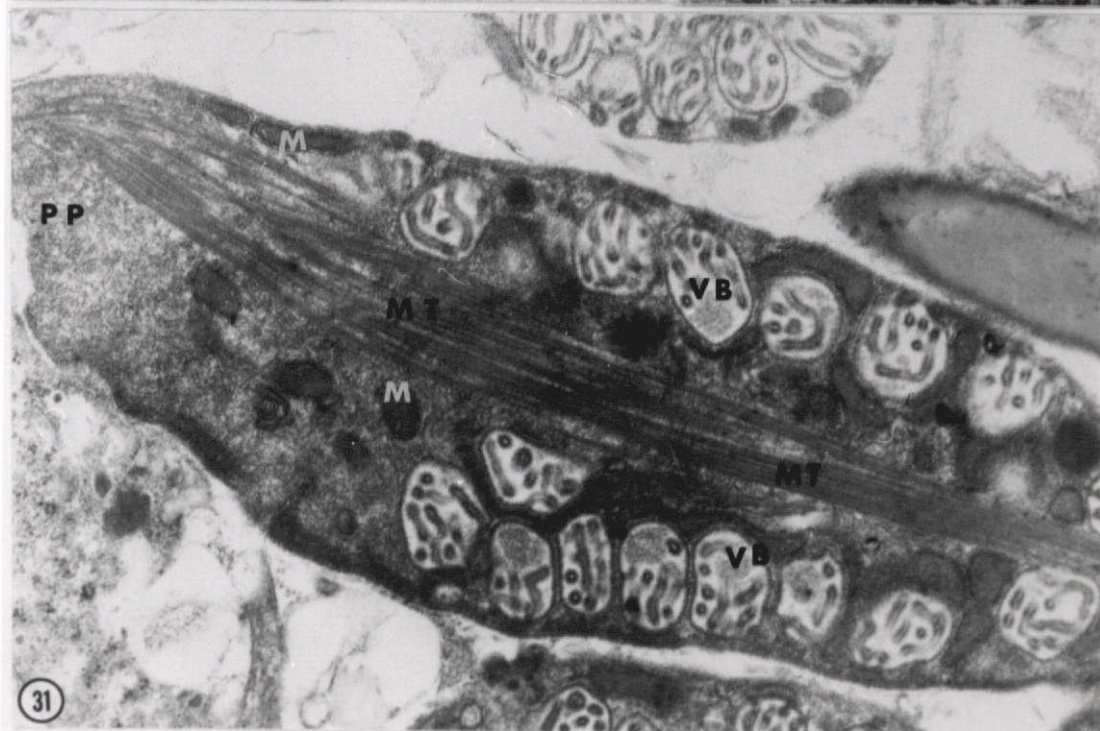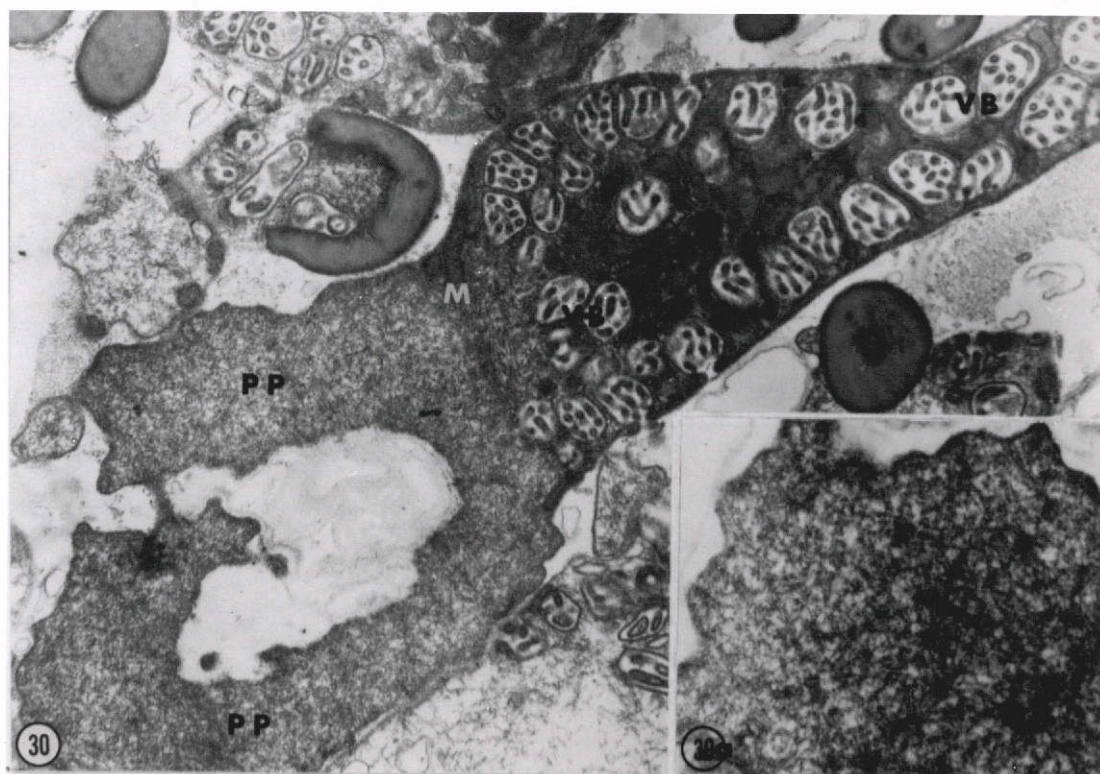
Fig. 30A. High magnification of amoeboid portion.

                                                          X 40,000

Fig. 31.   An electron micrograph showing microtubules (MY) running
           along the longitudinal axis of a sperm from the female.
           Vesicular bodies (VB), mitochondria (M), and a pseudopodium
           (PP) are shown.

                                                          X 20,000

Figs. 32 - 35

A series of electron micrographs illustrating changes in nuclear shape and structure during spermiogenesis. Nuclei (N), microtubules (white arrowheads), centrioles (C), mitochondria (M), vesicular bodies (FM), endoplasmic reticulum (ER), and a uterine wall (UW) are demonstrated.
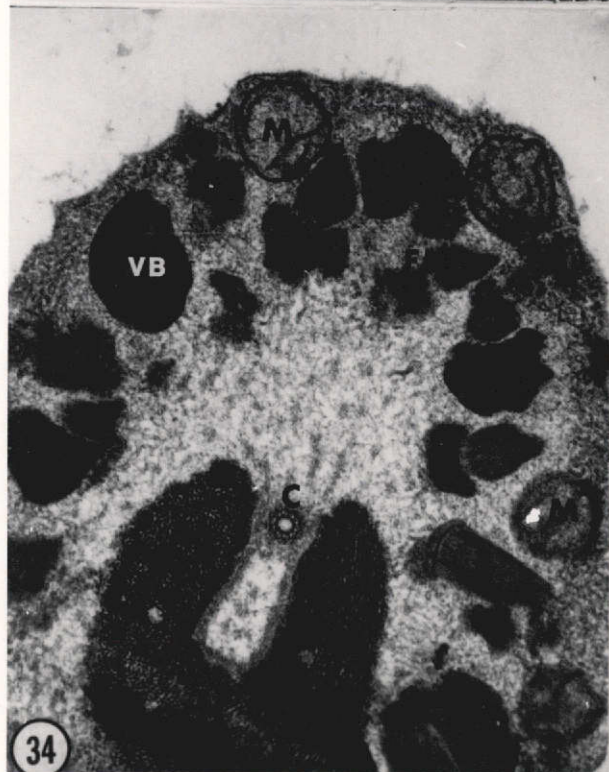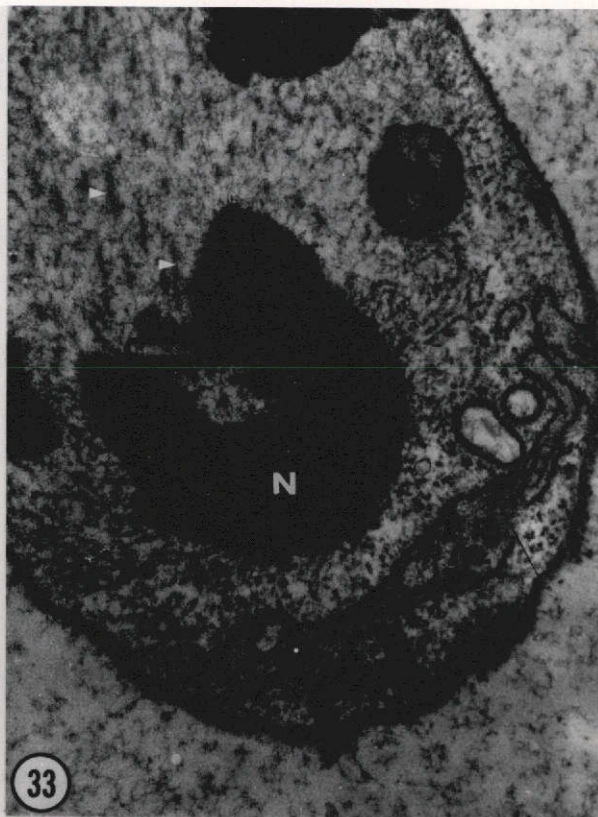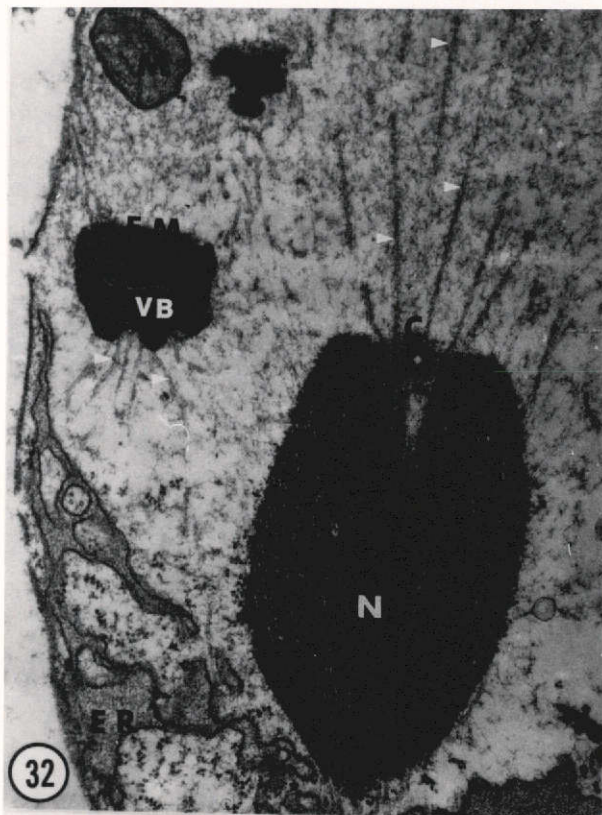
Fig. 32: X 16,000

Fig. 33: X 22,000

Fig. 34: X 31,000

Fig. 35: X 25,200

Figs. 36 - 40

A series of electron micrographs showing steps in vesicular
bodies differentiation. Fibrillar material (FM), hyper-
trophied portion (HP) of fibrillar body, inner membrane
invaginations (black arrowhead) in early vesicular body,
and vesicular bodies (VB) with collar-like thickenings
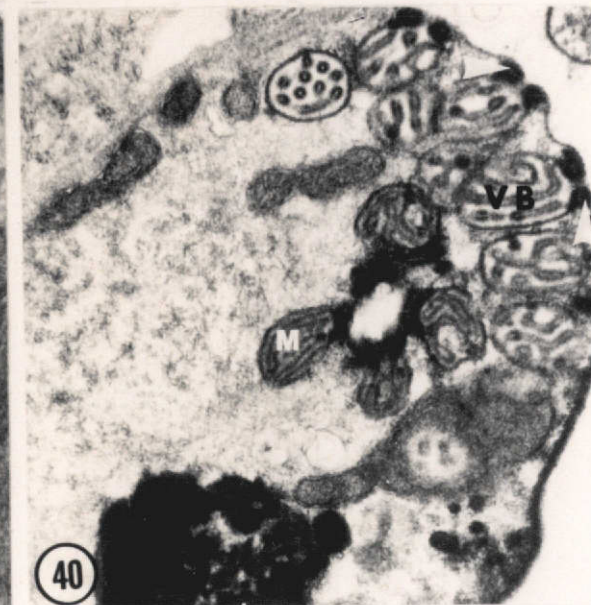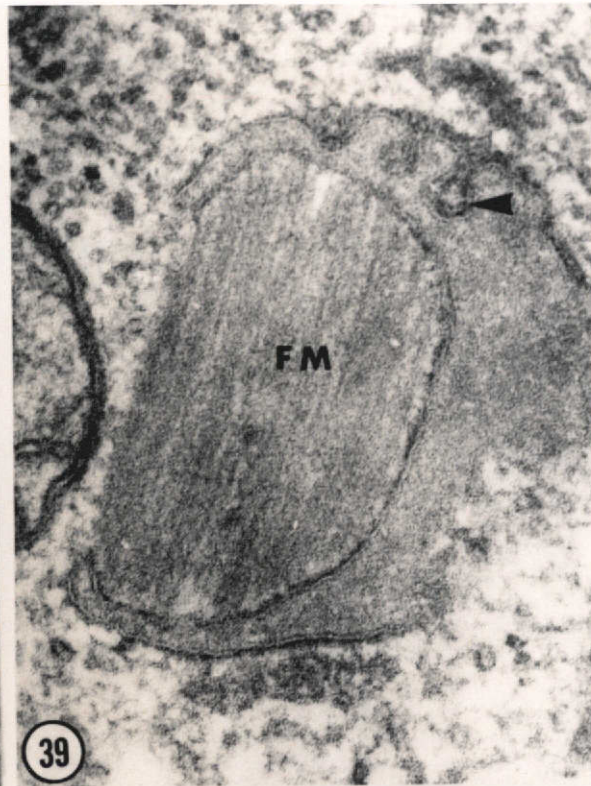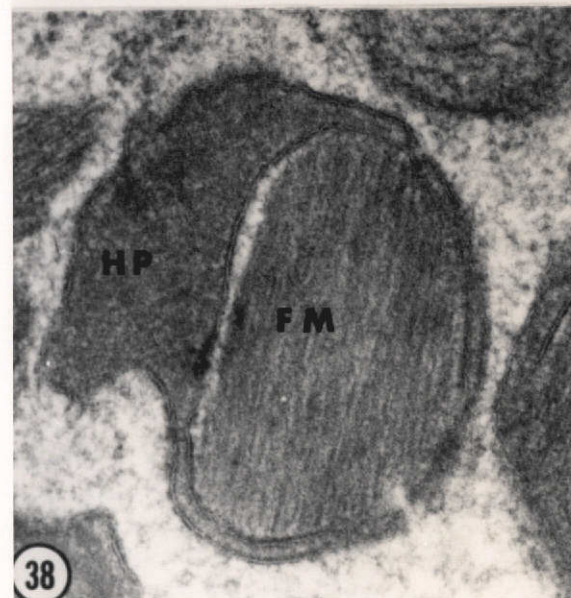(white arrowhead) are illustrated.
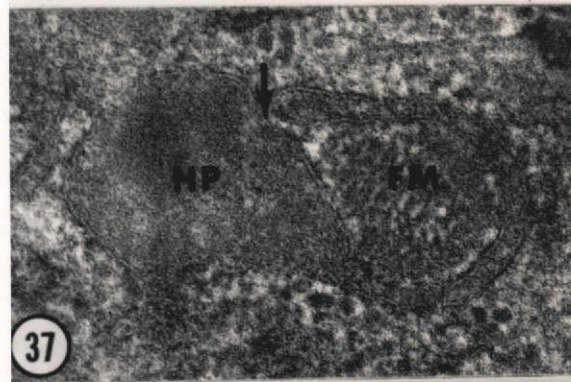
Fig. 36: X 20,000

Fig. 37: X 20,000

Fig. 38: X 34,000

Fig. 39: X 50,000

Fig. 40: X 9,600
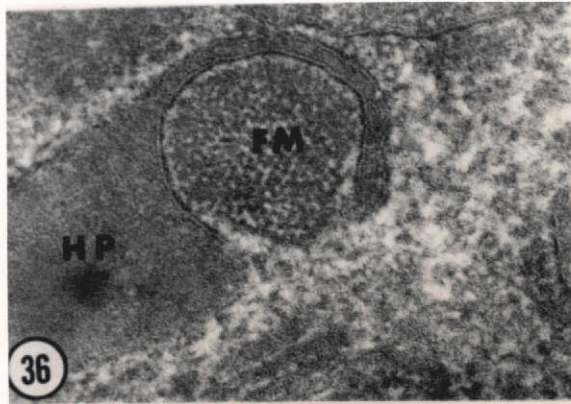
Fig. 41.   An electron micrograph of a sperm (SP) apposed to egg (EG)
           surface.   A nucleus (N), pseudopodial portion (PP),
           mitochondria (M), lipid droplet (L) are shown.   Arrows
           point to thickened vesicular projections of sperm vesicular
           bodies.

                                                      X 6,000

Fig. 42.   En electron micrograph of a sperm (SP) apposed to egg (EG)
           surface.   A decondensed nucleus (N), and thickened vesicular
           body projections (VP) are illustrated.   Lipid droplets (L)
           are shown in the egg (EG).

                                                      X 18,000
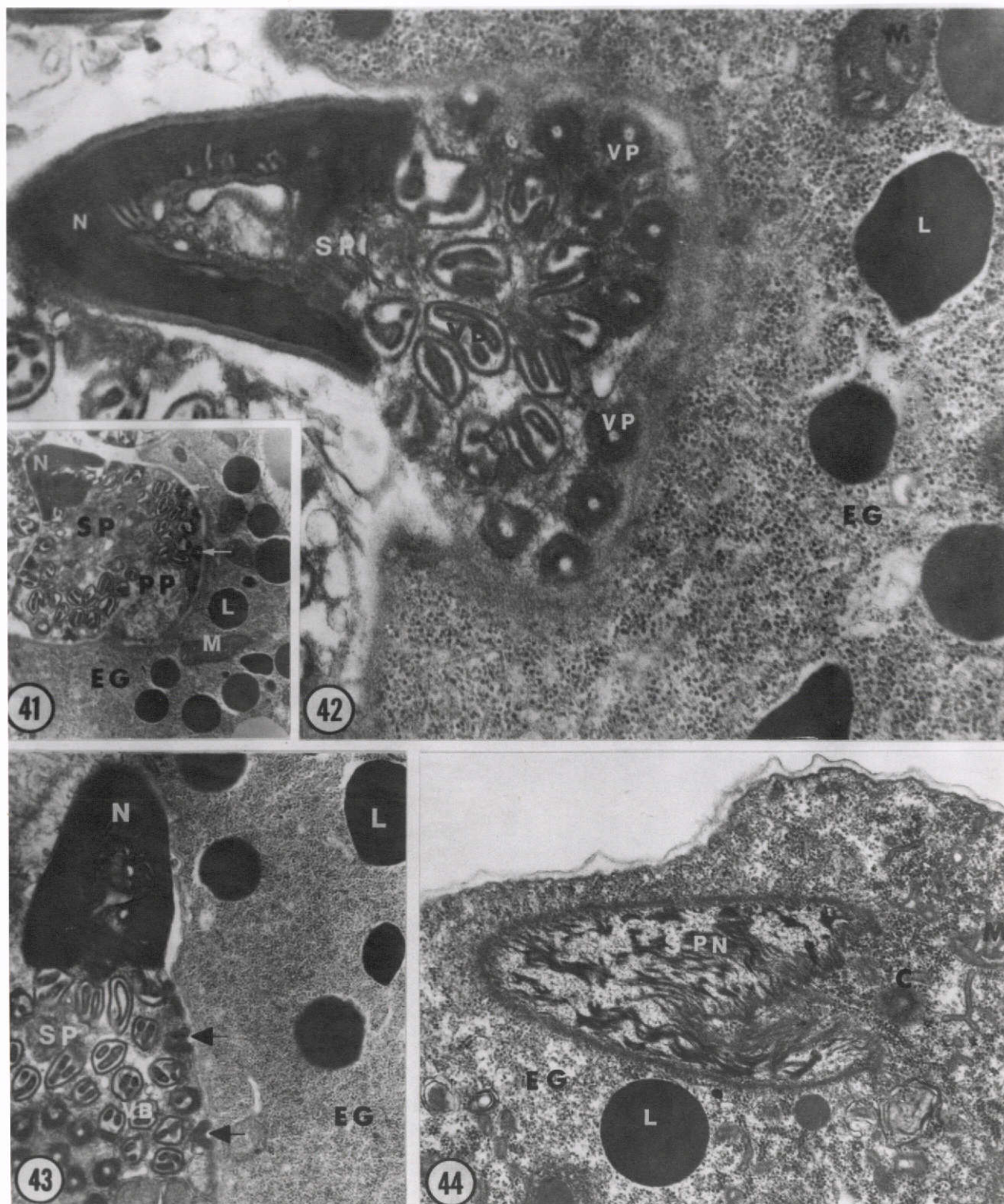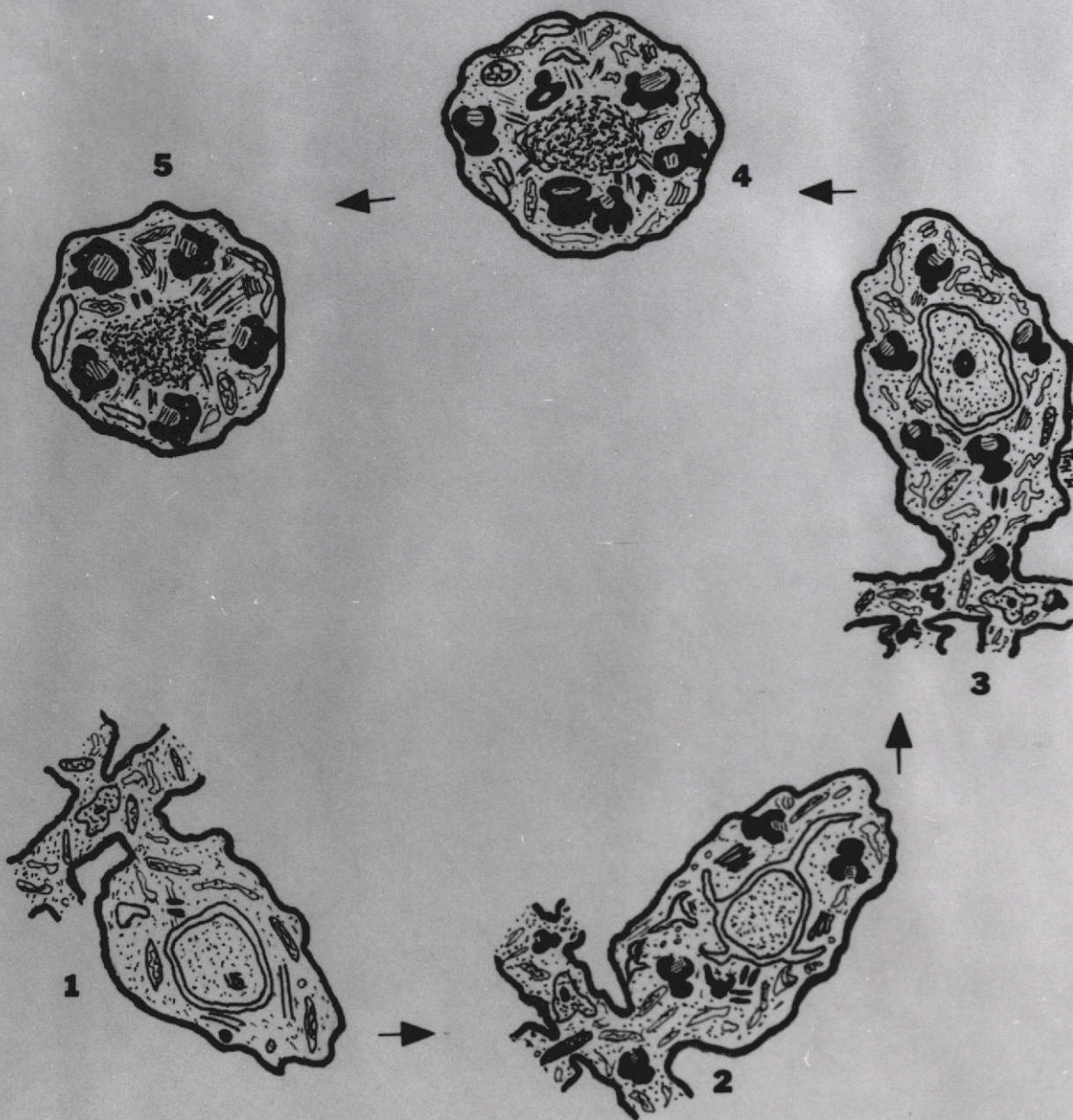
Fig. 43. A diagramatic summary of spermatid formation.
1= early spermatogonium; 2= advanced spermatogonium;
3= primary spermatocyte; 4= secondary spermatocyte;
5= spermatid.
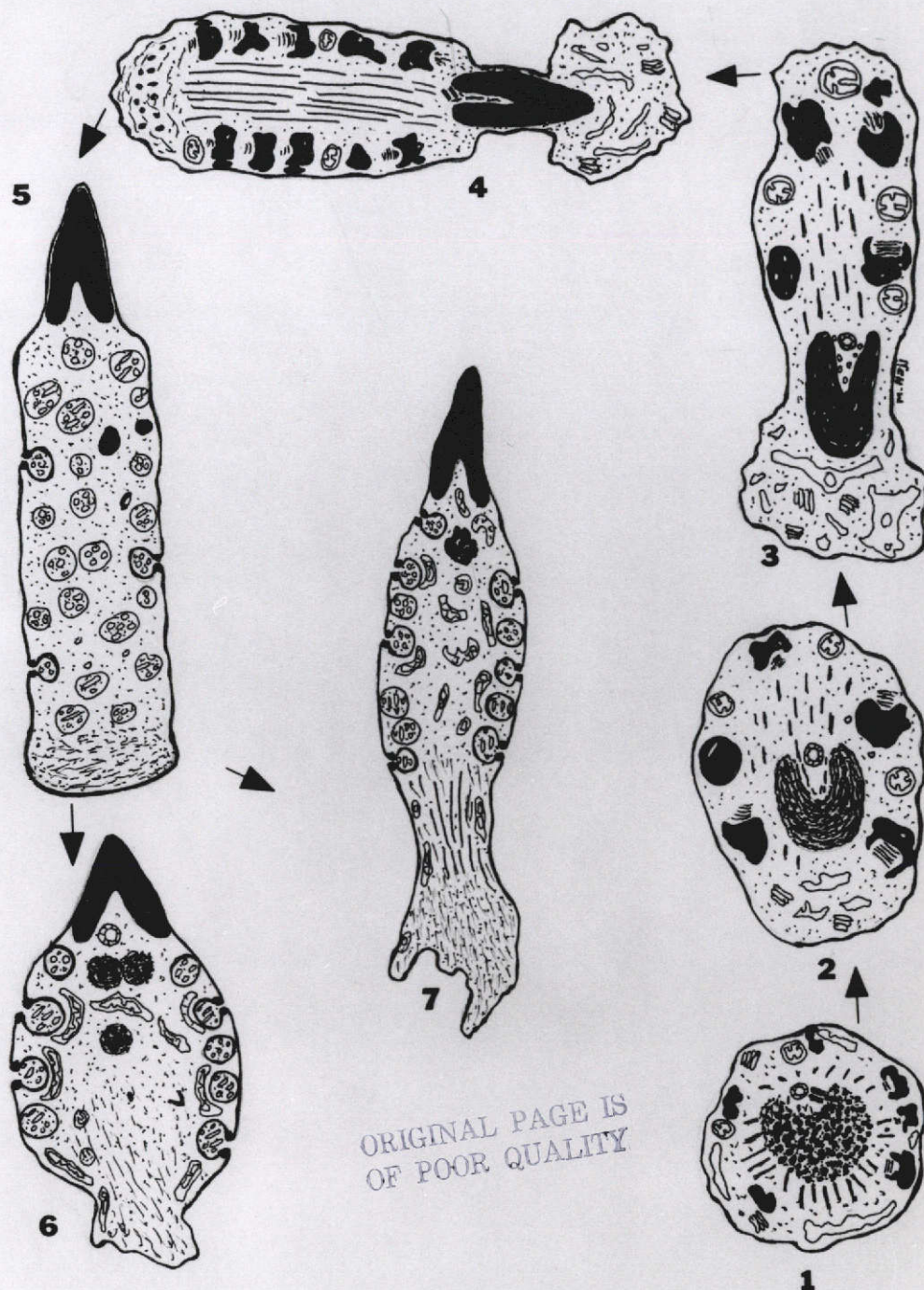
Fig. 44. A diagramatic summary of spermiogenesis.
1= young spermatid;
2= intermediate spermatid;
3= elongated spermatid;
4= elongated spermatid about to shed its cytophore;
5= sperm from seminal vesicle;
6= globular sperm from female genital tract;
7= elongated sperm from female genital tract.

REFERENCES

Beams, H. W., and Sekhon, S. S. (1972) Cytodifferentiation during genesis in Rhabditis pellio, J. Ultrastruct. Res. 38, 511-527.

Bishop, M. W. and Walton, A. (1966) Spermatogenesis and the Structure of Mammalian Spermatozoa. In N. Marshall's Physiology of Reproduction, Ed. by A. S. A. Parks, Vol. 1, Part 2 Pg. 1-129.

Cheng, T. C. (1964) The Biology of animal parasites: Aschelminthes. W. B. Saunders. Philadelphia.

Clark, W. H., Jr., Moretti, R. L. and Thomson, W. W. (1967) Electron microscopic evidence for the presence of an acrosomal reaction in Ascaris lumbricoides var. suum. Exp. Cell Res. 47, 643-647.

_____, Thomson, W. W., and Moretti, R. L. (1968) Electron microscopic and histochemical characterization of the proacrosomal vesicles found in the gametes of Ascaris lumbricoides var. suum. J. Cell Biol. 39, 252.

_____, Moretti, R. L., and Thomson, W. W. (1972) Histochemical and ultrastructural studies of the spermatids and sperm of Ascaris lumbricoides var. suum. Biol. of Reprod. 7, 145-159.

Cross, J. (1961) A modified method for the culture and isolation of larvae of intestinal nematodes. J. Parasitol. 47: 26.

Collier, V. (1937) Studies on the cytoplasmic components in fertilization. I. Ascaris suilla. Quart. J. Micros. Sci., 78, 397-418.

Dym, M. and Fawcett, D. W. (1971) Further observations on the numbers of spermatogonia. Spermatocytes and spermatids connected by intracellular bridges in the Mammalia testis, 4 (2): 195-215.

Favard, P. (1961) Evolution des ultrastructures cellulaires an cours de la spermatogenese de l'Ascaris. Ann. Sci. Nat. Zool. Ser. 12, 53-152.

Fawcett, D. W. (1961) Intercellular bridges. Exp. Cell Res. Sapp. 8, 174-187.

Foor, W. E. (1970) Zygote formation in Ascaris lumbricoides (Nematoda). J. Cell Biol. 39, 119-134.

_____ (1970) Spermatozoan and zygote formation in nematodes. Biol. Reprod. Suppl. 2, 159-176.

Foor, W. E., Johnson, M. H., and Beaver, P. C. (1971) Morphological changes in the spermatozoa of Dipetalonema vitae in utero. J. Parasit., 57 (6), 1163-1169.

_____, and McMahon, J. T. (1973) Role of the glandular vas deferens in the development of Ascaris spermatozoa. J. Parasit. 59 (5), 753-758.

_____. (1974) Morphological changes of spermatozoa in the uterus and glandular vas deferens of Brugia pahangi. J. Parasit., 60 (1), 125-133.

Franklin, L. E. (1971) An association of endoplasmic reticulum with the Golgi apparatus in golden hamster spermatids. J. Reprod. Fert., 27: 67-71.

Hyman, L. H. (1951) The invertebrates: Acanthocephala, Aschelminthes, and Entoprocta, Vol. III. "The Pseudocoelomate Bilateria". McGraw-Hill, New York.

Jamuar, M. P. (1966) Studies of spermiogenesis in a nematode Nippostrongylis brasiliensis. J. Cell. Biol., 31, 381-396.

Kanwar, U. (1971) Sperm cytoplasmic remnants in the Nematode Ascridia galli. J. Parasit., 57, 193.

Lee, D. L., and Anya, O. A. (1967) The structure and development of the spermatozoan of Aspicluris tetraptera (Nematoda). J. Cell Sci., 2, 537-544.

_____. (1971) The structure and development of the spermatozoan of Heterakis gallinarum (Nematoda). J. Zool., Lond., 164: 181-187.

Miller, M. J. (1966) Observations on spermatogenesis in Onchocerca volvulus and Wucheria bancrofti. Can. J. Zool., 44: 1003-1006.

Nath, V. (1956) Cytology of spermatogenesis. Int. Rev. Cytol., 5: 395-451.

_____, Gupta, B. L., Kochhar, D. (1961) The histochemistry of the male germ cells of the nematode Porrocaecum angusticolla, a parasite in the vulture. Quart. J. Micros. Sci., 102: 39-50.

_____, and Singh, S. (1956) The nematode sperm. Res. Bull. Punjab Univ., 91: 121-135.

Neil, B. W., Wright, K. A. (1973) Spermatogenesis in the hologenic testis of the trichuroid nematode, Capollaris hepatice. J. Ultrastruct. Res., 44: 210-234.

Panijel, J.   (1950)   Researches sur la nature et la signification de la proteine gram du gamete male d'Ascaris megalocephala. Biochim. Biophys. Acta, 6: 79-93.

Pasteels, J.   (1948)   Recherches surle cycle germinal chez l'Ascaris Etude cytochimique des acides nucleiques dems l'oogneese, las spermatogenese et le development chez Parascaris equorum Goeze. Arch. Biol. L (Leige), 59: 405-447.

Pasternak, J., and Samoiloff, M. R.   (1971)   Cytoplasmic organelles present during spermatogenesis in the free-living nematode Pansgrellus silusiae.   Can. J. Zool., 50: 147-151.

Romieu, M.   (1911)   La spermatogenese chez l'Ascaris megalocephala. Arch Zellforch., 6: 254-325.

Sommerville, R. I., and Weinstein, P. P.   (1964)   Reproductive behavior of Nematospiroides dubius in vitro and in vivo.   J. Parasit., 50 (3): 401-409.

Spurr, A. R.   (1969)   A low-viscosity eopoxy resin embedding medium for electron microscopy.   J. Ultrastruct. Res., 26: 31.

Sturdivant, H. P.   (1934)   Studies on the spermatocyte divisions in Ascaris megalocephala with special reference to the central bodies, Golgi complex, and mitochondria.   J. Morph., 55: 534-565.

Van Beneden, E., and Julin, C.   (1884)   La spermatogenese chez l'Ascaris megalocephalae.   Bull. Acad. Roy. Belg., 7: 312-342.

Venable, J. H., and Coggeshall, R.   (1965)   A simplified lead citrate stain for use in electron microscopy.   J. Cell Biol., 25: 507.

Wright, K. A., Hope, W. D., and Jones, N. O.   (1973)   The ultrastructure of the sperm of Deontostoma californicum, a free-living marine nematode.   Proceed. Helminthol. Soc. Wash., 40: 30-36.

2.   The effects of colchicine on the spermatids and sperm of

      Nematospiroides dubius.

INTRODUCTION

Several investigations have confirmed the inhibition of cer-
tain biological functions by the drug colchicine. This agent and its
derivatives have been reported to disrupt the microtubules of the mito-
tic spindle (Brinkley and Stubblefield, 1967; Picket-Heaps, 1967; Robins
and Gonatas, 1964), Radiolarian axopodia (Tilney, 1965), human neuro-
blasts (Seeds et al, 1970), and microtubules of other cell types (for
review see Margulis, 1973, Olmsted and Borisy, 1973; and Bryan, 1974).

Through investigations with microtubule depolymerizing agents,
like colchicine, different functions have been attributed to microtubules
in various cell types. Among these are the participation of microtubules
in development and maintenance of cell shape (Tilney, 1968; Warren, 1968;
Turner, 1970; Seeds et al, 1970; Hendel and Roth, 1971; Piatigorsky et
al, 1972; Daniels, 1972; Bouck and Brown, 1973). Other functions of
microtubules like chromosome movements in cell division, intracellular
organization and movement of material, cellular motility, and cellular
transduction have been reported and are reviewed by Olmsted and Borisy
(1973), Margulis (1973), and Bryan (1974).

In the preceding chapter the longitudinal orientation of micro-
tubules during spermatogenesis of N. dubius sperm has been reported, and
an important role for microtubules in sperm differentiation was suggested.
Only two reports have dealt with the effect of colchicine on spermato-
genesis (Turner, 1970 and Wright, 1968). Turner (1970) reported the
loss of flagellar and microtubular sheaths in colchicine treated Nitella
spermatids, and the branching of flagella of treated sperm. Wright
(1968) found that nuclear elongation did not take place during spermio-
genesis in the spermatid of Uma inornata if colchicine was present.
In view of the known effects of colchicine, and the virtual lack of
information on the impact of this agent on invertebrate sperm dif-
fernetiation, the present investigation was undertaken.

MATERIALS AND METHODS

Mature N. dubius males were isolated from the duodenum of infected male mice and kept in 37°C, 0.85% NaCl (Sommerville and Weinstein, 1964). Reproductive tracts were released from the body of the male worm by making a cut about 3 mm anterior to the bursae. A group of 10 seminal vesicles (and other portions of the male reproductive system) were placed in a control medium of 0.85% NaCl, and a similar group was treated with colchicine (Sigma Chemical Company) prepared in 0.85% NaCl at 10 mN concentration, pH 7.3. The colchicine was protected from light before use. Both control and colchicine treated samples were placed in a water bath at 37°C for 6 hours. The tissues incubated in colchicine were tested for recovery by transferring them to a control medium for 5 hours.

Control and treated samples were examined with a Nomarski phase contrast microscope. For electron microscopy, the samples were fixed in 3% glutaraldehyde buffered with 0.1 M phosphate buffer at pH 7.3 or a 0.1 M calodylate at pH 7.3. In all instances 6% sucrose was added. The tissues were postfixed with 1% osmium tetroxide in 0.1 M phosphate or 1.0 M cacodylate buffer at 4°C for 1 hour. After dehydration in an acetone series, the samples were embedded in Spurr's epoxy resin (1969). Ultrathin sections were mounted on 300-mesh undercoated grids, and stained with alcoholic uranyl acetate followed by lead citrate (Venable and Coggeshall, 1965). Sections were examined with an AEI-EM 6B or an Hitachi H-S-8 electron microscope.

RESULTS

Light Microscopy:

Untreated Cells:

In untreated tissues, about 90% of the cells exhibit the characteristic cylindrical body form with a "V" shaped nucleus at one pole and

a cap-like pseudopodial region at the opposite pole. Along the sperm surface, bead-like structures (vesicular bodies) are observed (Fig. 1). The terms anterior and posterior will be used to refer to the pseudopodial and nuclear portions respectively.

Colchicine Treated Cells:

A smear of seminal vesicles treated with 10 mM colchicine and examined with a phase contrast microscope demonstrates sperm with different forms as illustrated in Figs. 4-9. The changes in shape first occur about 5 hours after suspension in colchicine. Those regions of the sperm which appear to be most sensitive to this agent are posterior to the pseudopodial areas (Figs. 4, 5), and the ones least affected are anterior to the nuclear region (Figs. 4, 5). However, after 6 hours of incubation in colchicine, the area anterior to the nucleus is also affected (Figs. 6-9). As illustrated various degrees of bending occur at the sperm surface as well as localized areas of swelling and constriction (Figs. 6-9) The nuclear shape and position do not appear to be affected (Figs. 4-9); however, the pseudopodial portion loses its normal shape. The cap-like appearance of the pseudopod is lost, swelling is pronounced, and in some cases small processes are seen projecting from it (Figs. 5-9). The vesicular bodies appear to be of the same size and distribution as those of the control (Figs. 1, 4-9).

Recovery of Treated Cells:

The effects of 6-hour exposure to colchicine on sperm shape are slowly reversible. When seminal vesicles treated with colchicine for 6 hours were transferred to a control medium for 5 hours, signs of recovery were observed. Usually no change in sperm shape was noticed during the first 3 hours after transfer. After 4 hours, recovery was first observed in the area anterior to the nucleus (Fig. 2), and 5 hours later in the pseudopodial portion (Fig. 3).

Electron Microscopy:

Untreated Cells:

A detailed description of untreated N. dubius sperm has been presented in the previous chapter. Briefly, elongated spermatids and sperm have longitudinally oriented microtubules in the central cytoplasm which otherwise lacks organelles. Vesicular bodies with finger-like invaginations along the peripheral cytoplasm, electron dense "V" shaped nuclei with no nuclear envelope, and cap-like pseudopodial poles which contain filaments and dense sites believed to be microtubule termination points are other traits of control cells. Some of these features are demonstrated in Fig. 10.

Colchicine-treated Cells:

Gametes from seminal vesicles exposed to 10 mM colchicine for 6 hours exhibit disassembly of microtubules. Elongated spermatids have an inner cytoplasmic portion void of microtubules and the portion of the cells anterior to the nucleus is swollen (Fig. 11). The vesicular bodies look similar to those of control cells (Fig. 10), in that they have inner membrane invaginations in their hypertrophied portions, and appear to have extruded their fibrillar component (Figs. 10, 11). Vesicular bodies of treated and control sperm are similar and show granular material on the surface of, and in between their inner finger-like projections (Figs. 12-15).

Along the longitudinal axes, some areas look constricted, and bending is usually associated with these areas (Fig. 13). The position, structure and shape of nuclei do not appear to be affected by colchicine. In all observed cases the nuclei are electron dense, and polar in position (Figs. 12, 13).

The pseudopodial ends have undergone pronounced bending. In some cases, the inner pseudopodial margin fuses with the adjacent surface of the cell (Figs. 13, 15, 17). Also, appearance of lateral pseudopodial projections and lack of microtubules in the vicinity of this sperm pole are evident (Figs. 15-17).

Recovery of Treated Cells:

Seminal vesicles suspended in colchicine for 6 hours and transferred to control media for 5 hours contained cells, of which 80% showed signs of recovery. As illustrated in Fig. 20, few microtubules are evident in the vicnity of pseudopodial areas. The reappearance of microtubules coincides with the regeneration of normal morphology. Also, there is a noticeable lack of constrictions along the surface of recovered sperm (Figs. 18, 20).

DISCUSSION

In the previous chapter the author reported the radial arrangement of microtubules around the nuclei of young spermatids and the parallel orientation of these structures along the longitudinal axes of elongated spermatids. In addition, it was hypothesized that these microtubules were responsible for certain aspects of morphogenesis and the maintenance of N. dubius sperm shape. The results of the present investigation lend support to the second of these hypotheses. This is evident by the fact that sperm treated with colchicine do not maintain their normal morphology. These results are in agreement with those of Yamada et al (1971), and Brown and Bouck (1973) which implicate microtubules in maintenance of cell shape.

The regeneration of normal shape of N. dubius colchicine-treated sperm demonstrates that the action of this agent is reversible. Similar results have been reported in Actinosphaerium (Tilney, 1968), Chlamydomonas (Rosenbaum et al, 1969), and in other cell systems. Borisy and Taylor (1967) and other authors suggested that the mechanism of colchicine action is to bind microtubular dimers which apparently prevents reassembly of the subunits and leads to depolymerization of existing microtubules.

The finding that the anterior pseudopodial area of the sperm is first affected by the action of colchicine suggests that the microtubules are depolymerized in the pseudopodial area initially with

subsequent propagation of this depolymerization toward the nucleus. The observation that recovery is first noticed in the nuclear zone of the sperm and later in the pseudopodial area lends further support to this suggestion. In a detailed study, Brown and Bouck (1973) reported that microtubules close to Ochromonas beak nucleating sites were assembled first with subsequent repolymerization from these sites. Although it is not yet known if the reassembly of microtubules after depolymerization is unidirectional or random (Olmsted and Borisy, 1973), recent reports (Granett et al, 1973) have described unidirectional "growth" of microtubules when isotopically labelled chick brain microtubules were used as seeds. The pattern of loss and recovery of N. dubius sperm shape described in this report suggests that depolymerization and reploymerization of microtubules occur in a unidirectional fashion.

As Borisy et al (1974) reported, the polarity of tubule assembly is pertinent to the concept of nucleation. In this connection, Porter (1966) pointed out that because microtubules are associated with shape changes in different cells, spatial and temporal patterns of microtubule initiating sites probably exist. Such sites have been reported by several investigators (Picket-Heaps, 1969; Tilney, 1970; Brown and Bouck, 1973; Allen and Borisy, 1973). Since the microtubules appear to originate from the nuclear fossa of the sperm of N. dubius, it seems likely that the centrioles, which lie in the fossa, are responsible for tubule assembly.

The present experiments have demonstrated that microtubules are essential in maintenance of sperm morphology. However, these experiments have not clarified the role microtubules may play in sperm development. Long-term exposure to colchicine, necessitating organ culture of the seminal vesicle, will be necessary to answer this question.

Fig. 1. A light micrograph of a control sperm suspended in 0.85%
         NaCl for 6 hours. A nucleus (N1), a pseudopodial cap (PC),
         and vesicular bodies (arrows) are shown.   X 2,700

Fig. 2. A light micrograph of a sperm suspended in 10 mM colchicine
         for 6 hours and transferred to a control medium for 4 hours.
         Nucleus (N), pseudopodial cap (PC), and vesicular bodies
         (white arrows) are demonstrated. Arrow shows bending in
         pseudopodial portion.   X 2,700

Fig. 3. A light micrograph showing a completely recovered sperm
         originally placed in a 10 mM colchicine solution for 6
         hours and then transferred to a control medium of 0.85%
         NaCl for 5 hours. A nucleus (N), vesicular bodies (white
         arrows), and a pseudopodial end (P) which has lost its
         cap-like appearance are shown.   X 2,700

Fig. 4. A light micrograph of a sperm suspended in 10 mM colchicine
         for 5 hours. The nuclear (N) appearance is normal. Swelling
         (white arrow) and constriction (black arrows) are evident,
         pseudopodial area (P) looks distorted.   X 2,200

Fig. 5. A light micrograph of a sperm suspended in 10 mM colchicine
         for 5 hours. Notice constriction (arrow), abnormal
         appearance of the pseudopodium (P) which has a lateral process
         (open triangle).   X 2,700

Fig. 6. A light micrograph of a sperm suspended in 10 mM colchicine
         for 6 hours. Bending in the pseudopodial area (arrowhead)
         and nuclear region (arrow), and swelling in between the two
         areas are evident. Also, a lateral pseudopodial process
         (open triangle) is shown.   X 2,700

Fig. 7. A light micrograph of a sperm suspended in 10 mM colchicine
         for 6 hours. Bending in the nuclear zone (arrow) and
         pseudopodial zone (arrowhead) are evident. Notice swelling
         in region enclosed between arrowhead and arrow. A nucleus
         (N) and a pseudopodium (P) with a small process (open triangle)
                  are shown.   X 2,700

Fig. 8. A light micrograph of a sperm cultured in 10 mM colchicine
         for 6 hours. Bending in pseudopodial area (arrowhead) and
         anterior to nuclear region (arrow), swelling between arrow
         and nucleus (N), and a lateral process (open triangle) from
         the pseudopodium (P) are demonstrated.   X 2,700

Fig. 9. A light micrograph of a sperm kept in 10 mM colchicine for
         6 hours. Loss of normal pseudopodial portion (P), appearance
         of lateral psudopodial process (open triangle), and bending
         (arrowhead and arrow) are shown.   X 2,700
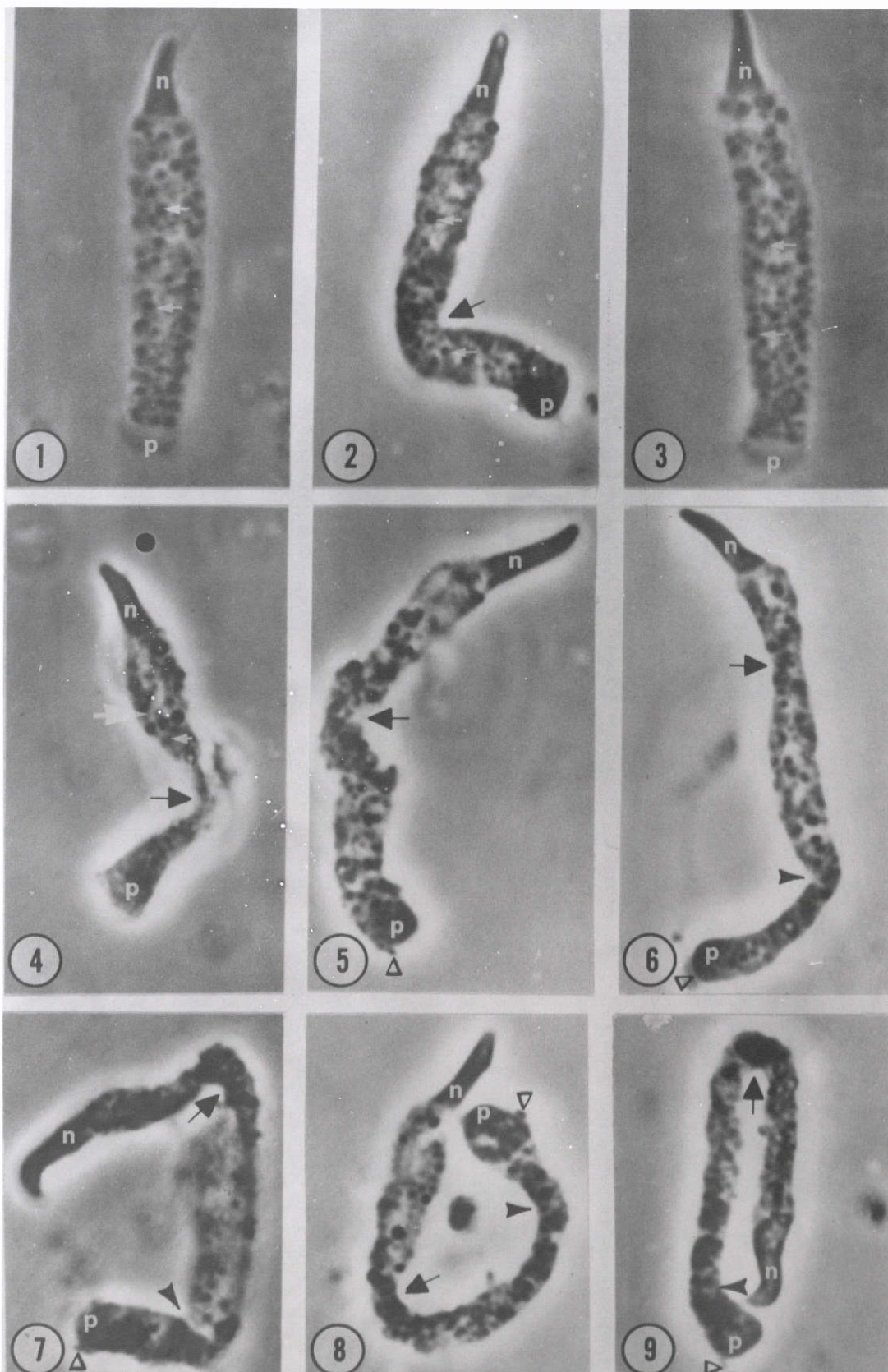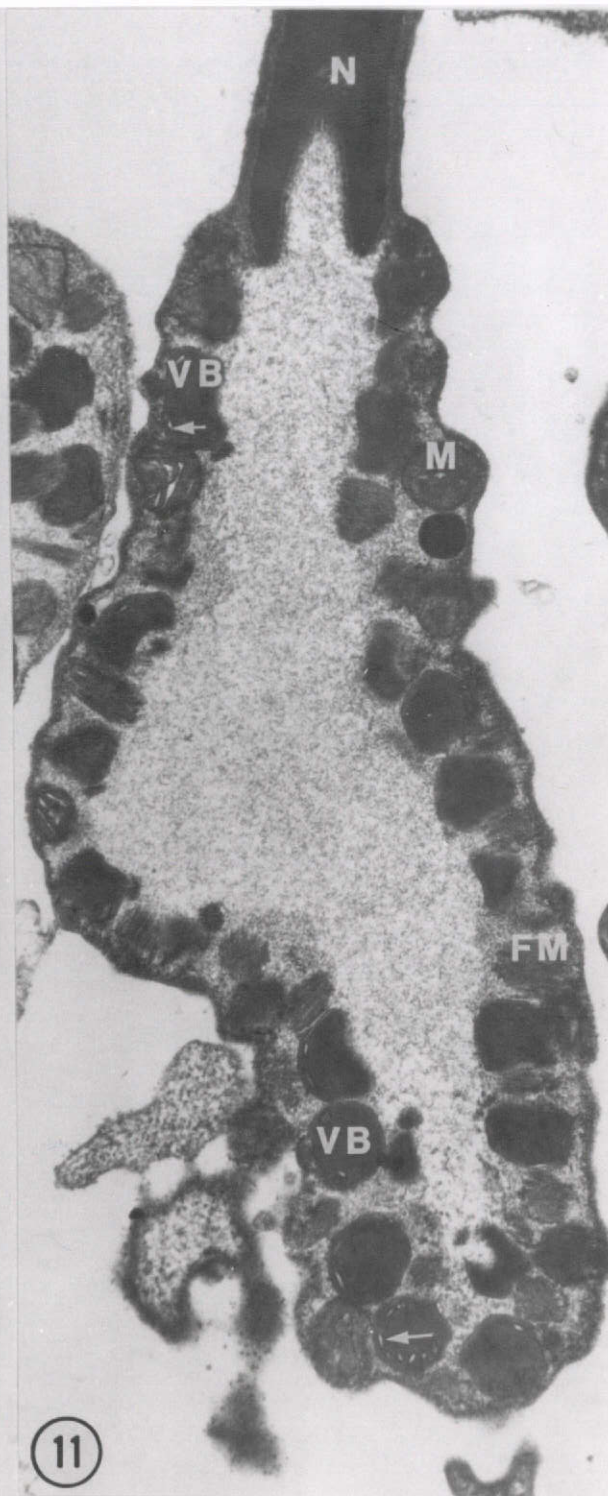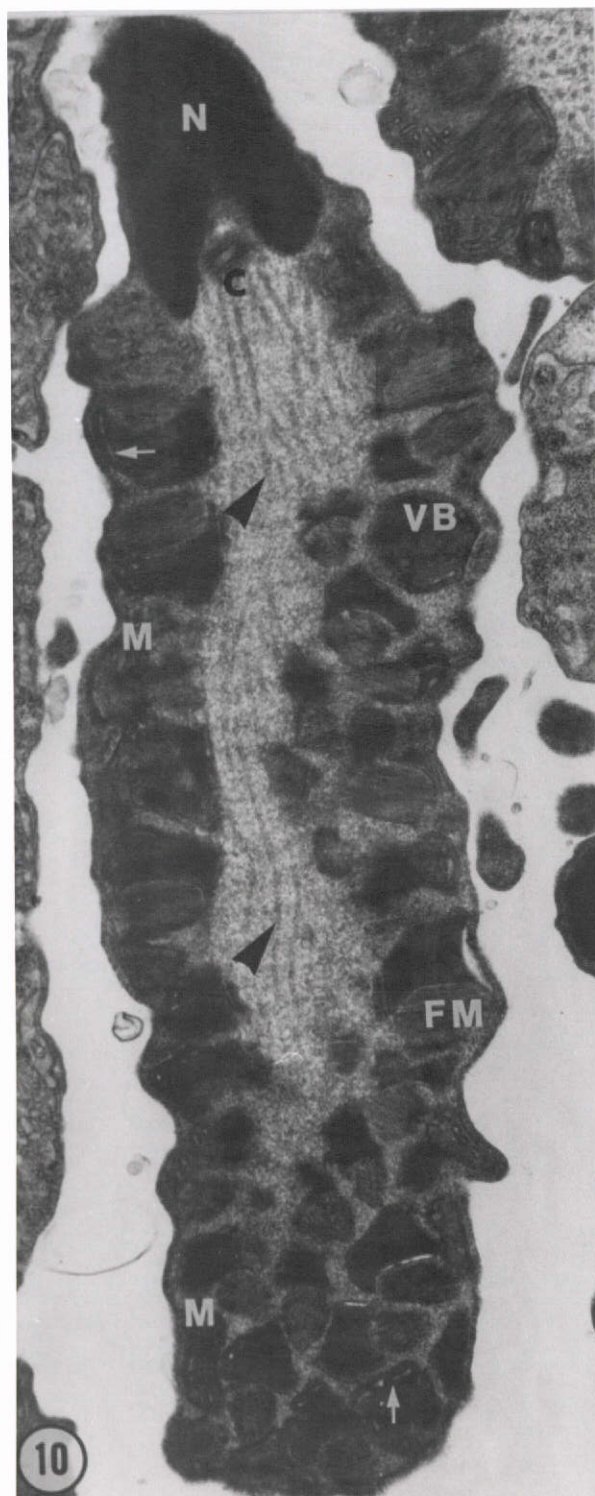
Fig. 10.   An electron micrograph of a control elongated spermatid
           cultured in 0.85% NaCl for 6 hours. A nucleus (N), a
           centriole (C), microtubules (arrowhead), vesicular bodies
           (VB) with inner membrane invaginations (small arrow) and
           extruded fibrillar material (FM) are demonstrated.

                                                         X 1,500

Fig. 11.   An electron micrograph of a spermatid cultured in 10 mM
           colchicine solution for 6 hours. Notice lack of micro-
           tubules. Vesicular bodies (VB) with inner membrane in-
           vagination (small arrow) and extruded fibrillar material
           (FM), nucleus (N), and mitochondria (M) are illustrated.

                                                         X 15,000

Fig. 12. An electron micrograph of a control sperm cultured in 0.85%
NaCl for 6 hours showing an electron dense nucleus (N),
vesicular bodies (VB) with inner finger-like projections,
lipid-like droplets (L), and a cap-like pseudopodia area
(PP). Large arrows point at dehiscing vesicular bodies.

X 14,000

Fig. 13. An electron micrograph of a sperm cultured in 10 mM colchicine
for 6 hours. Black arrows point at a constriction along the
sperm surface. White arrows show points of fusion of
pseudopodial membrane with adjacent sperm plasmalemma. A
nucleus (N), vesicular bodies (VB) with inner projections,
mitochondria (M) and lipid-like bodies (L) are shown.

X 15,000
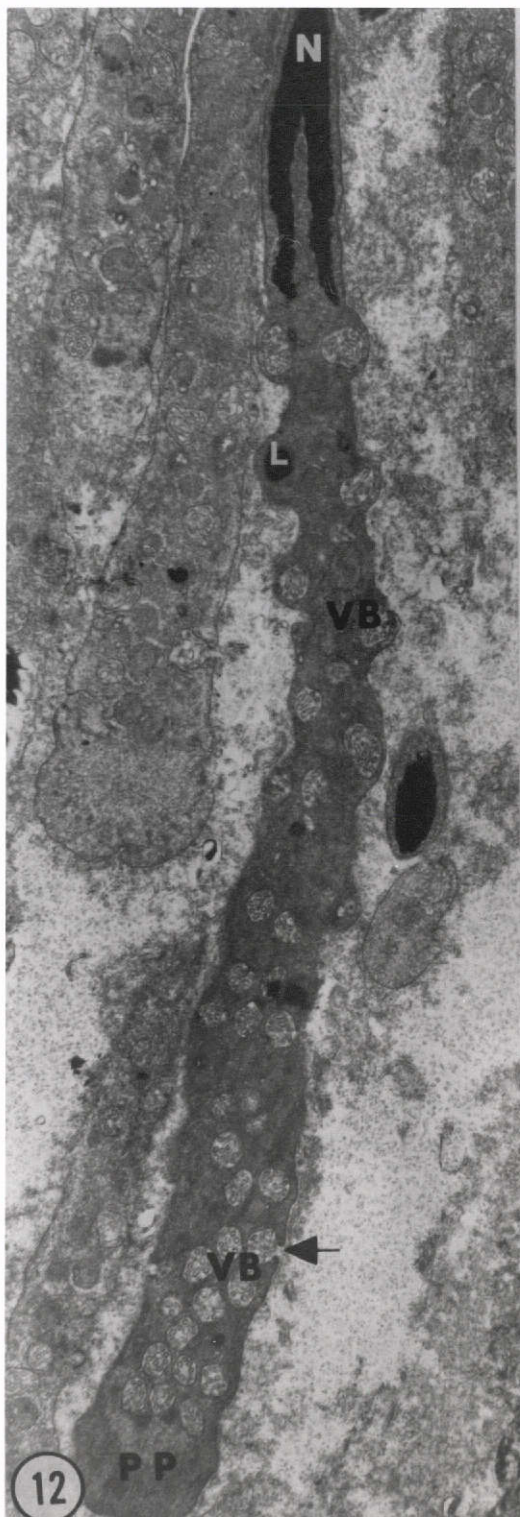
Fig. 14. An electron micrograph showing pseudopodial (PP) cap-like
          portion of a control sperm. Notice microtubules (white
          arrows) in the vicinity of the pseudopodial area. Vesicular
          bodies (VB) with inner finger-like projections are demonstrated,
          black arrows point at dehiscing vesicles.   X 20,000

Fig. 15. An electron micrograph illustrating the pseudopodial area of
          a sperm treated witn 10 mM colchicine for 6 hours. Notice
          bending of pseudopodial cap (arrowhead) and lack of micro-
          tubules. Vesicular bodies (VB) with inner finger-like pro-
          jections and mictochondria (M) are shown. Large arrow
   points to a dehiscing vesicular body.   X 21,000
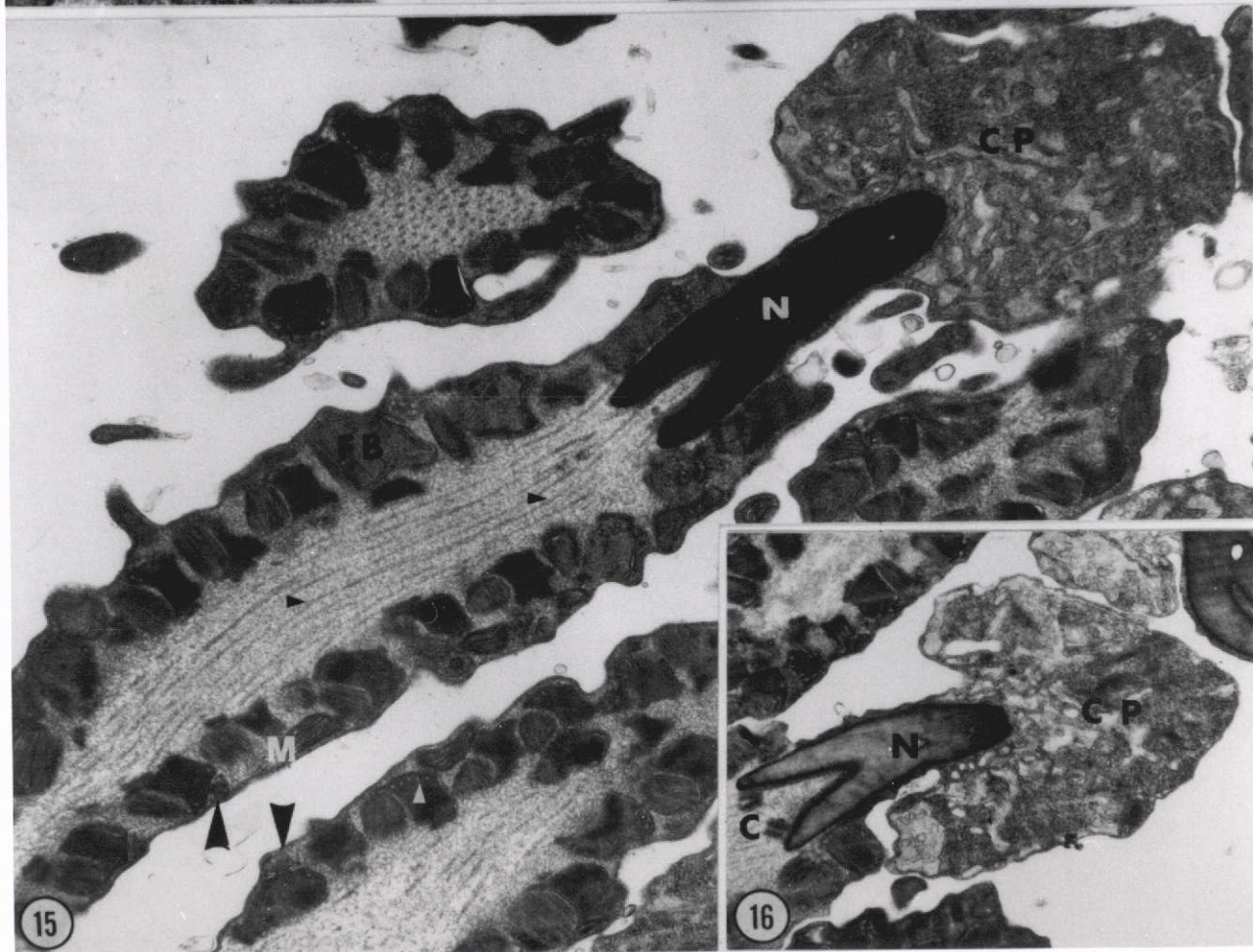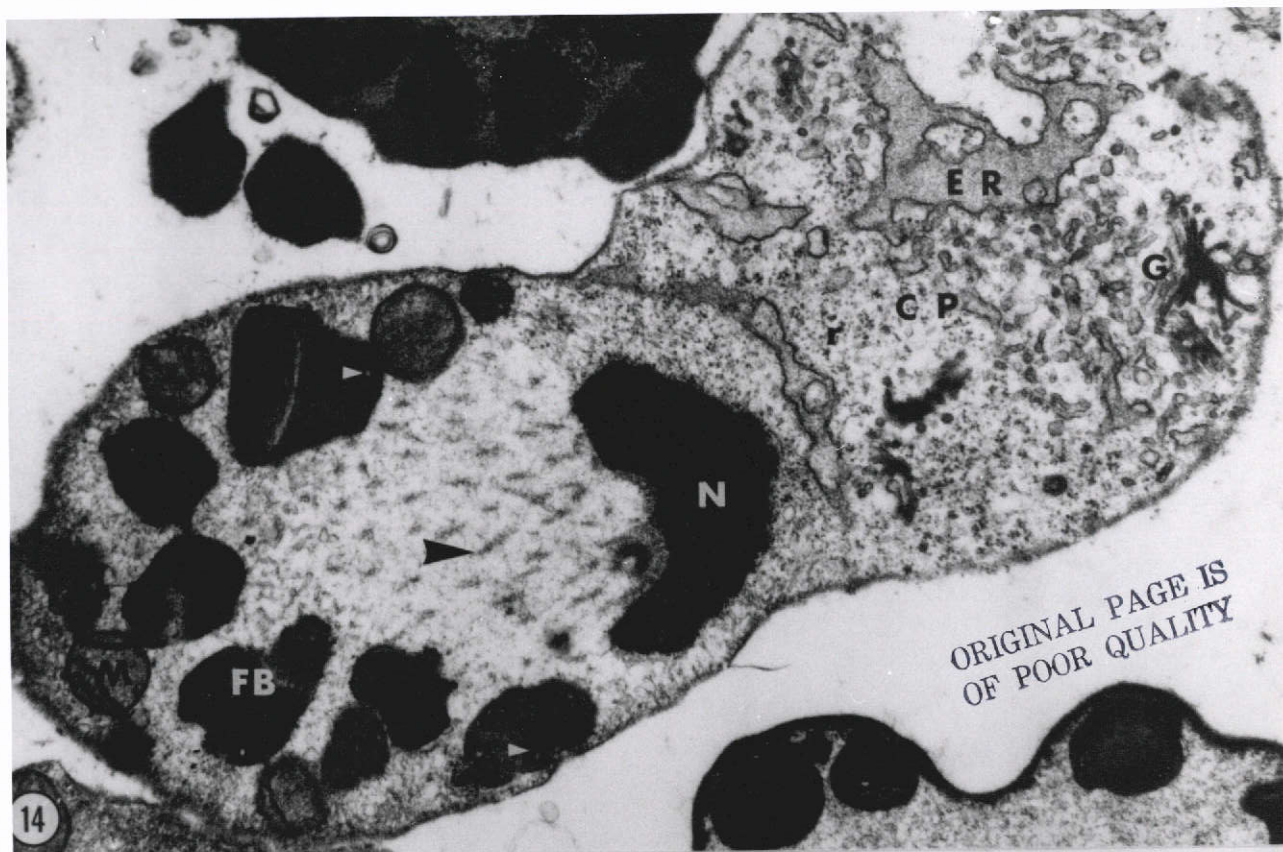
Figs. 16 and 17.

Electron micrographs of sperm incubated in 10 mM colchicine
solution for 6 hours. Constriction (arrows) and bending
are pronounced. Small processes are shown projecting from
pseudopodium (arrowheads, Fig. 16), and fusion of pseudo-
podial limiting membrane with plasmalemma (arrowheads, Fig. 17)
are illustrated. Vesicular bodies (VB) and mitochondria (M)
are shown. Fig. 16: X 18,000; Fig. 17: X 18,000
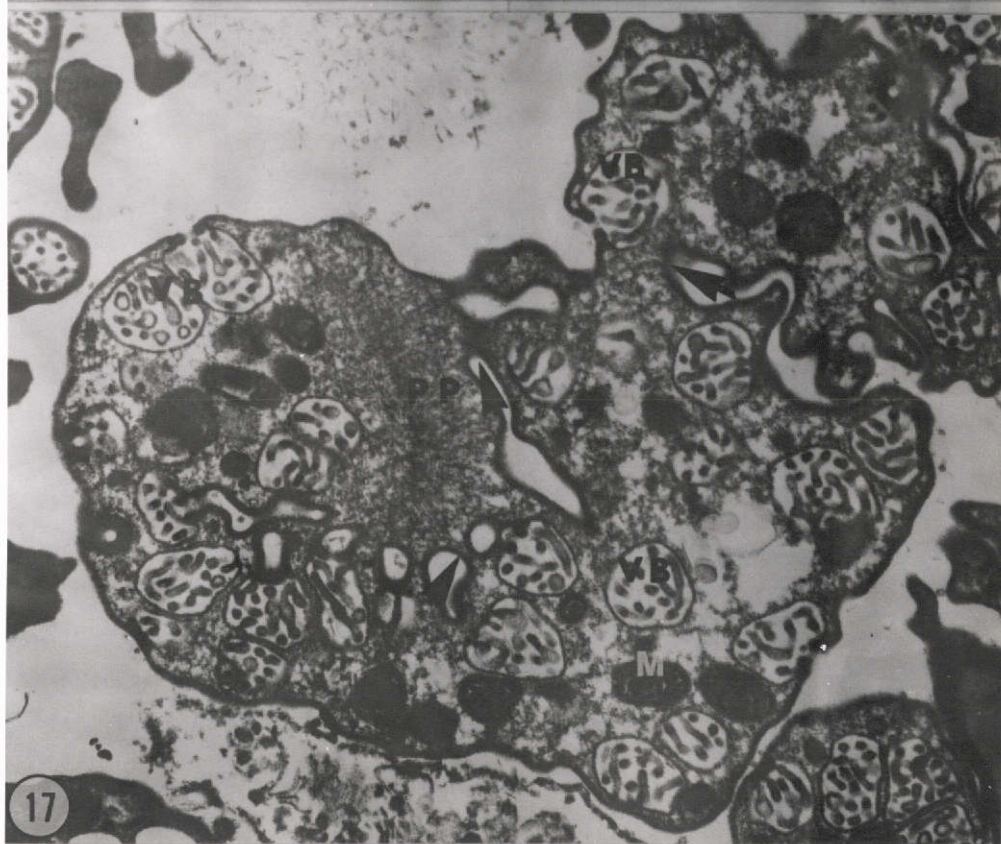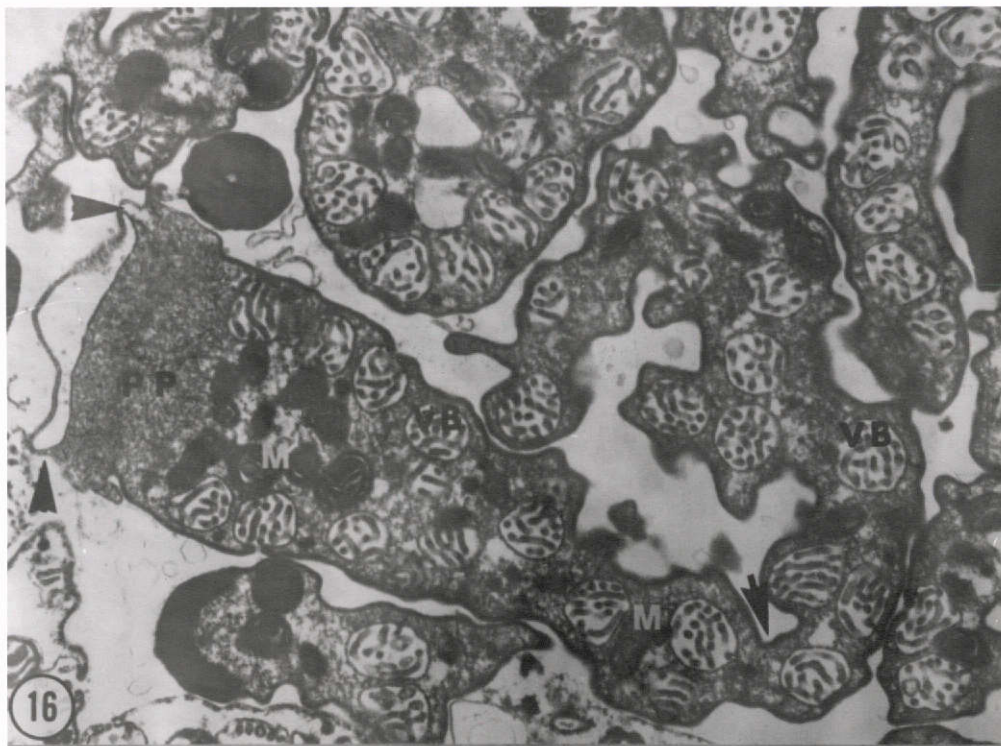
Fig. 18. An electron micrograph of a sperm treated with 10mM colchicine
for 6 hours and transferred to a control medium for 5 hours.
An electron dense nucleus (N), vesicular bodies (VB), lipid-
like droplet (L), and a cap-like pseudopodium (PP) are
shown.   X 14,000

Fig. 19. A light micrograph of a recovered sperm, demonstrating a
nucleus (N), a pseudopodial region (PP), and vesicular
bodies (arrows).   X 1,800

Fig. 20. An electron micrograph of the anterior portion of a recovered
sperm. Vesicular bodies (VB) which are dehiscing in some
cases (large arrows), few microtubules (small arrows), and a
pseudopodial portion (PP) are illustrated.   X 16,000
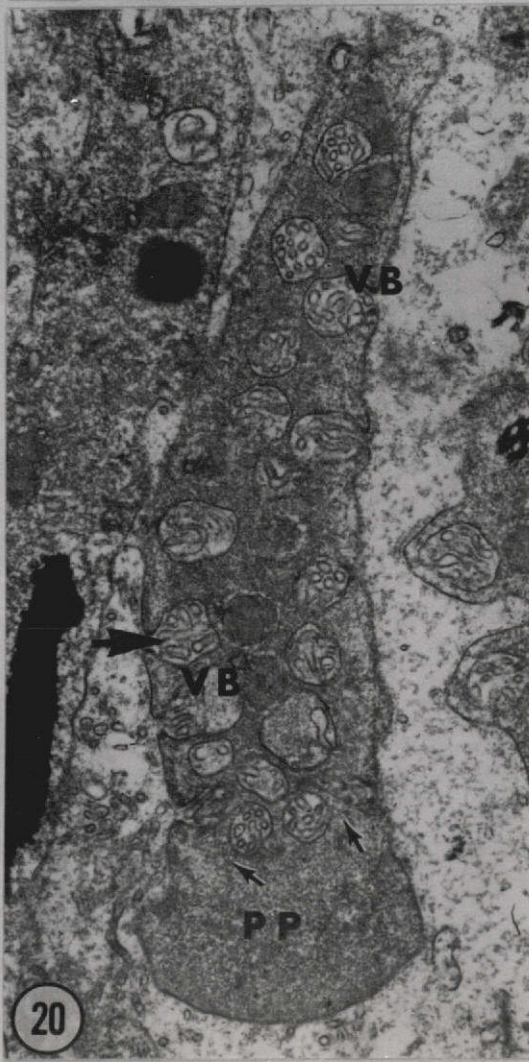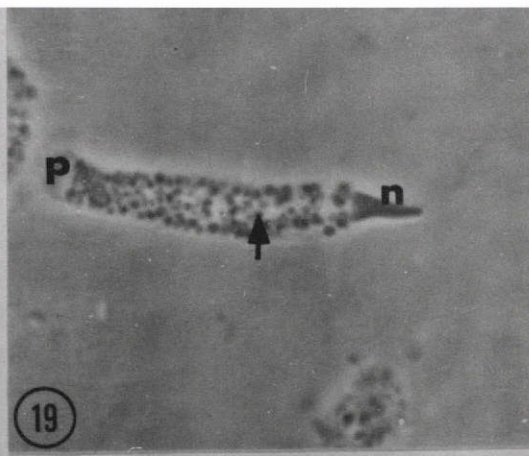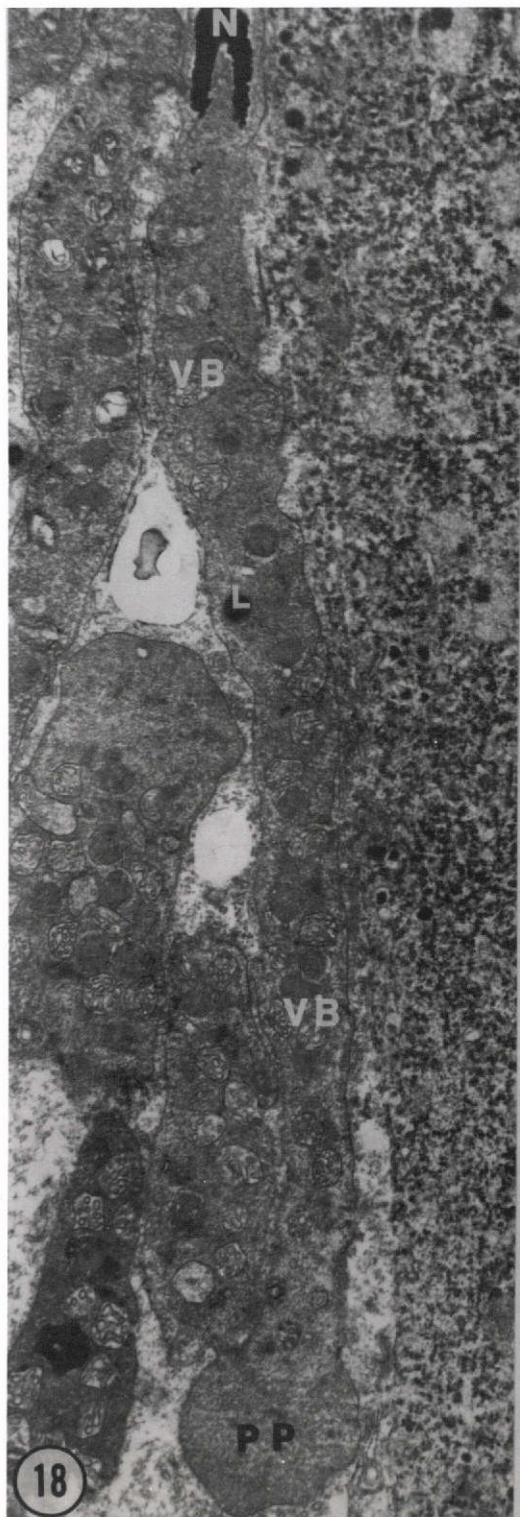
REFERENCES

Allen, C., and Borisy, G. 1973. Flagellar assembly in Chlamydomonas
in vitro addition of microtubule subunits to isolated axo-
nemes. J. Cell Biol., 59: 5a.

Behnke, O. 1970. A comparative study of microtubules of disk-shaped
blood cells. J. Ultrastruct. Res., 31: 61-75.

Binder, I. et al. 1973. Directionality of assembly of brain tubulin
onto flagellar axonemes. J. Cell Biol., 59: 24a.

Borisy, G. G., and Taylor, E. W. 1967. The mechanism of action of
colchicine. Binding of colchicine -3H to cellular protein.
J. Cell Biol., 34: 525.

Borisy, G. G. et al. 1974. Microtubule assembly in vitro. Fed.
Proceed., 33: 167-174.

Brinkley, B. R. et al. 1967. The effects of colcemid inhibition and
reversal on the fine structure of the mitotic apparatus of
chinese hamster cells in vitro. J. Ultrastructure Res., 19: 1.

Brown, D., and Bouck, G. 1973. Microtubule biogenesis and cell shape in
Ochromonas. II. The role of nucleating sites in shape
development. J. Cell Biol., 56: 360-378.

Bryan, J. 1974. Biochemical properties of microtubules. Fed.
Proceed., 33: 152-157.

Daniels, M. 1972. Colchicine inhibition of nerve fiber formation in
vitro. J. Cell Biol., 53: 164-176.

Goldman, R. D. 1971. The role of three cytoplasmic fibers in BHK-21
cell motility. I. Microtubules and the effects of
colchicine. J. Cell Biol., 51: 752.

Hendel, M. A., and Roth, L. E. 1971. Cell shape and morphology of the
neural tube: implications of microtubules function. Develop.
Biol., 25: 78-95.

Margulis, L. 1973. Colchicine-sensitive microtubules. Internal. Rec.
Cytol., 43: 333-361.

Olmsted, J., and Borisy, G. 1973. Microtubules. Ann. Rev. Biochem.,
42: 507-540.

Piatigorsky, J. et al. 1972. Cell elongation in the cultured embryonic
lens epithelium with and without protein synthesis. Involve-
ment of microtubules. J. Cell Biol., 55: 83-92.

Picket-Heaps, J. D. 1967. The effects of colchicine on the ultra-
structure of dividing plant cells, xylem wall differentiation
and distribution of cytoplasmic microtubules. Develop. Biol.,
15: 206.

Robbins, E., and Gonatas, N. K. 1964. Histochemical and ultrastructural
studies on Hela Cell cultures exposed to spindle inhibitors
with special reference to the interphase cell. J. Histochem.
12: 704.

Rosenbaum, J. L. 1969. Flagellar elongation and shortening in
Chlamydomonas. The use of cycloheximide and colchicine to
study the synthesis and assembly of flagellar proteins. J.
Cell Biol., 41: 600.

Seeds, N. W. et al. 1970. Regulation of axon formation by clonal lines
of a neural tumor. Proceed. Natl. Acad. Sci., 66: 160-167.

Sommerville, R. I., and Weinstein, P. P. 1964. Reproductive behavior
of Nematospiroides dubius in vitro and in vivo. J. Parasit.
50: 401-409.

Spurr, A. R. 1969. A low viscosity epoxy resin embedding medium for
electron microscopy. J. Ultra. Res., 26: 31-43.

Tilney, L. G. 1968. Studies on the microtubules in heliozoa. The
effect of colchicine on the formation and maintenance of
the axopodia and the redevelopment of pattern in
Actinosphaerium nucleofilm (Barrett). J. Cell Sci., 3: 549.

Tilney, L. G., and Gibbins, J. R. 1969. Microtubules in the forma-
tion and development of primary mesenchyme in Arbacia
punctulata. II. An experimental analysis of their role in
development and maintenance of cell shape. J. Cell Biol.,
41: 227.

Turner, E. 1970. The effects of colchicine on spermatogenesis in
Nitella. J. Cell Biol., 46: 220-234.

Venable, J. M., and Coggeshall, K. 1965. A simplified lead citrate
stain for use in electron microscope. J. Cell Biol., 25:
407-408.

Warren, R. 1968. The effects of colchicine on myogenssis in vitro
in Rana pipiens and Rhodnius prolixus (Hemiptera). J. Cell.
Biol., 39: 544-555.

79.

Wright, S. 1968. Studies on spermiogenesis in the lizard Uma
inormata. Ph.D. Dissertation, University of California,
Riverside.

Yamada, K. M. et al. 1971. Ultrastructure and function of growth
cones and axons of cultured nerve cells. J. Cell Biol.
49: 614.